Supplement of

Performance Characterization of Low-Cost Sensor Observations During Long-Term Deployments in North Carolina and Rural Malawi

Ashley S. Bittner et al.

Correspondence to: Ashley S. Bittner (asbittne@ncsu.edu)

S1 Details of monitoring equipment

The ARISense sensor package is shown in Figure S1; see Cross et al. (2017) for full description. Version 2.0 added a GSM cell module and replaced the Ox-B421 with the Ox-B431 sensor (Alphasense Ltd., UK). The ARISense sensor packages used AC or DC power and drew 3 – 4 W on average. In rural Malawi, units relied on a DC power system of four 9-Watt solar panels and four 12,000mAh rechargeable batteries; batteries were in a separate weather-proofed housing with a single bus connected to the ARISense unit. Raw data were sampled every 60 seconds, integrated, and stored as daily data files on an internal USB drive. During deployment in Malawi, data files were periodically sent via email or uploaded to a shared Google Drive by an on-site local assistant using an Android phone.

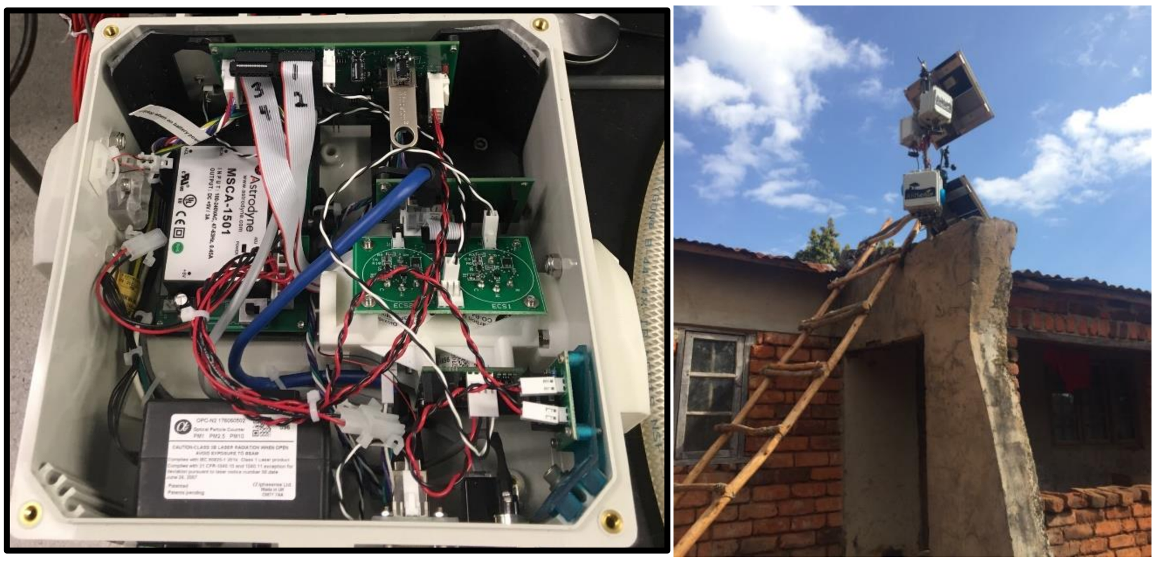

Figure S1: Image of ARISense (Version 1.0) interior (left), including integrated circuit board and internal data logging system. Image of ARISense in deployment setting (right) with solar panel power system mounted at Village 2 site in Mulanje, Malawi.

The MicroPEM uses a proprietary software to provide real-time mass concentration estimates from the nephelometer. We did not apply any correction factors and the internal slope was set to 1. The filters were equilibrated in a climate-controlled weighing chamber for 24 hours (22 ± 2 °C, 35 ± 2.5 % RH) and charge neutralized with Polonium and electrostatic ionization sources prior to pre- and post-weighing on an ultramicrobalance (Mettler Toledo UMX-2, 0.1 µg readability). Field handling blanks (N= 3) were collected in Malawi and were used to correct the gravimetric $PM_{2.5}$ concentrations. During field data collection, the filters were stored in sealed containers and were wrapped in foil to minimize exposure to light. The filters were stored in a refrigerator while in Malawi (when possible) and in the freezer after returning to the U.S. While in transit, the filters were at ambient temperature. The field blank-corrected gravimetric filter mass concentrations were used to post-correct the nephelometer readings.

S2 Details of pre-collocation in North Carolina

This study was conducted in 2017, before standardized protocols were developed. The variable collocation periods used in this study were constrained by equipment malfunction, limited field personnel in Malawi, and international travel timelines. Recent U.S. EPA guidelines for supplemental air sensor performance assessment suggest 1) a minimum of 30 days (720 hours) of collocation, 2) two collocations during two different climatic seasons OR at two different sites, 3) a 24-hour averaging interval for the sensor and reference data, and 4) a 75% completeness requirement (Duvall et al., 2021a, b).

Figure S2: Image of ARISense at reference monitoring site (left) and Google Earth aerial image of location of Triple Oak monitoring site, Morrisville, North Carolina, 27560 USA. Image source: © Google Earth 2021. Google Earth Version 9.143.0.0 (May 1, 2018). *NC Collocation Site, Durham, NC, USA*. 35.865°N, 78.820°W. Borders and labels; places layer. Accessed: August 19, 2021. NC DEQ link to data available from: https://xapps.ncdenr.org/aq/ambient/AmbtSiteEnvista.jsp?site=371830021

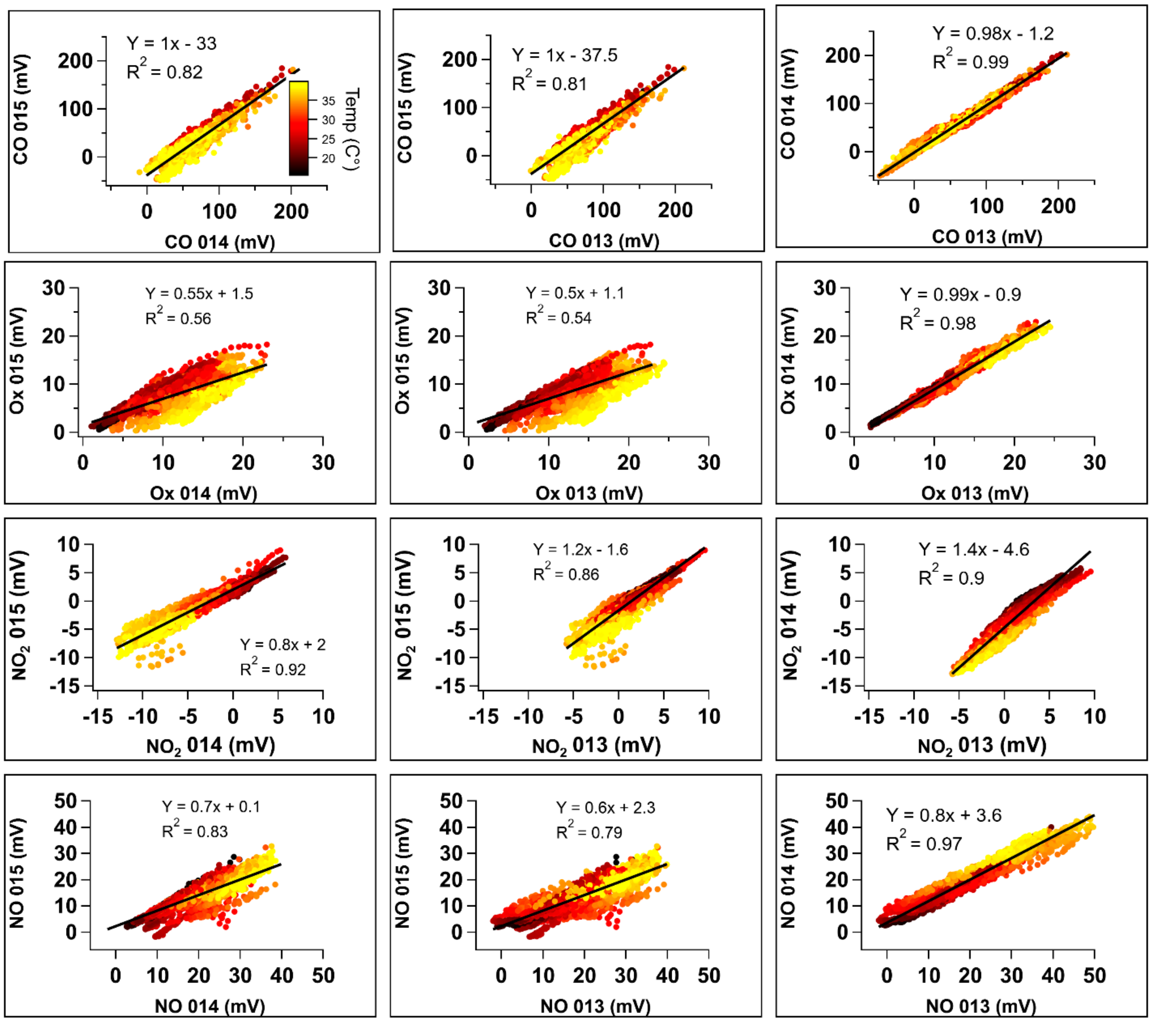

Figure S3: Scatter plots of raw differential voltage data from each gas sensor (rows) in each monitor pair (columns) during pre-collocation in NC. Linear fit coefficients (y = mx + b) and the Coefficient of Determination (R^2) are shown for each monitor-monitor gas sensor pair. Data points are colored by ambient temperature.

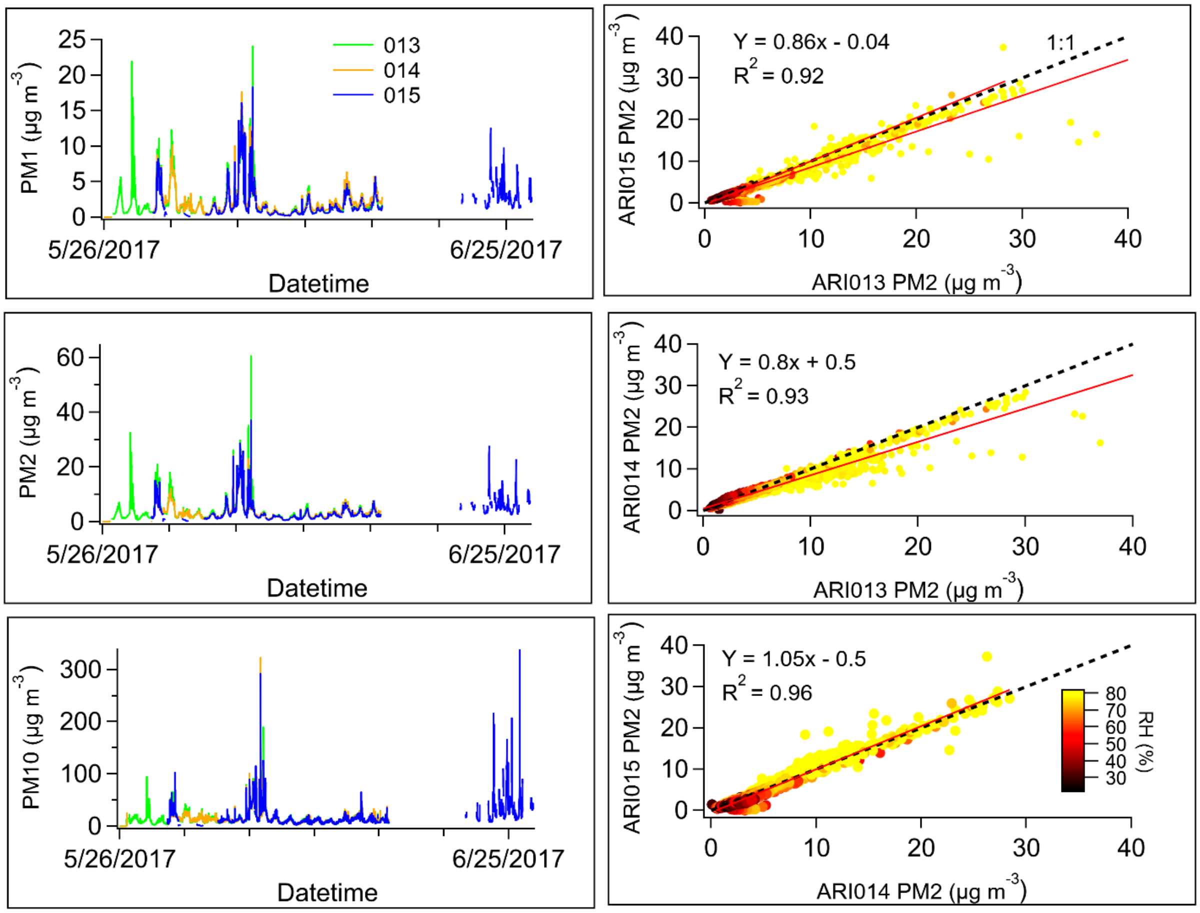

Figure S4: Time series of PM_1, $PM_2.5$ and PM_{10} mass concentration measurements from ARI013, ARI014, and ARI015 during pre-deployment collocation in North Carolina (left); Line color indicates ARISense unit number. Scatter plots of $PM_{2.5}$ mass concentration measurements from ARI013, ARI014, and ARI015 (right). Point color indicates relative humidity conditions. Linear regression coefficients (y = mx + b), fit line (red line), and the Coefficient of Determination (R^2) are shown for each paired comparison; A one to one comparison line is shown as the dotted black line.

S3 Details of OPC-N2 Collocation in Malawi

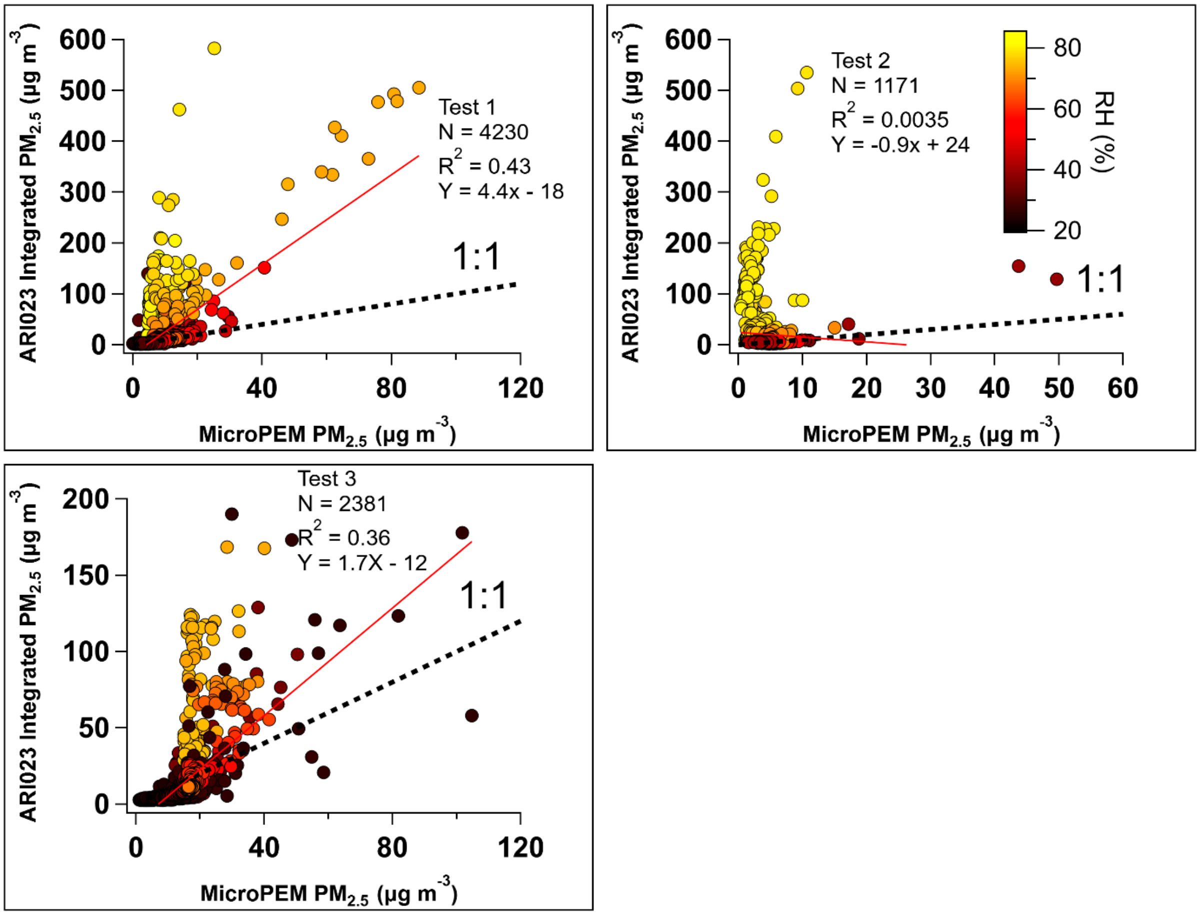

Figure S5: Scatter plots of uncorrected $PM_{2.5}$ mass concentration measurements from the Alphasense OPC-N2 sensor in ARI023 compared to measurements made by the mass-corrected MicroPEM nephelometer during collocation in Malawi. Three tests were conducted over 130 hours. Point color indicates relative humidity conditions. Linear regression coefficients (y = mx + b), fit line (red line), and the Coefficient of Determination (R^2) are shown for each paired comparison; A one to one comparison line is shown as the dotted black line.

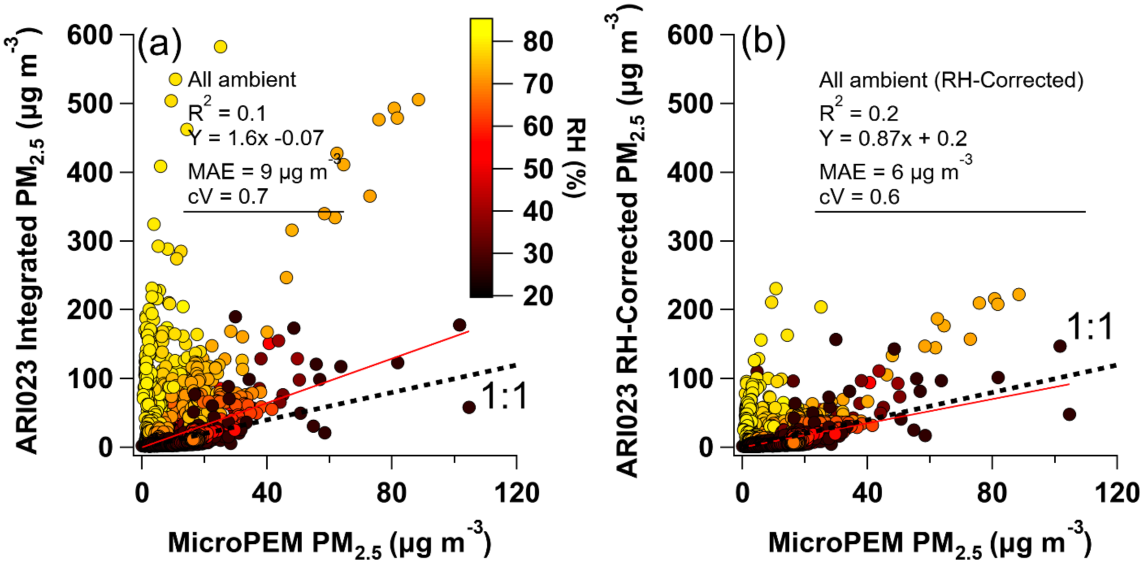

Figure S6: Scatter plots of (a) uncorrected and (b) RH-corrected $PM_{2.5}$ mass concentration measurements from the Alphasense OPC-N2 sensor in ARI023 compared to measurements made by the mass-corrected MicroPEM nephelometer during collocation in Malawi (1-min resolution). Point color indicates relative humidity conditions. Linear regression coefficients (y = mx + b), fit line (red line), the Coefficient of Determination (R^2), mean absolute error (MAE), and the coefficient of variation (cV) are shown for each paired comparison; A one to one comparison line is shown as the dotted black line.

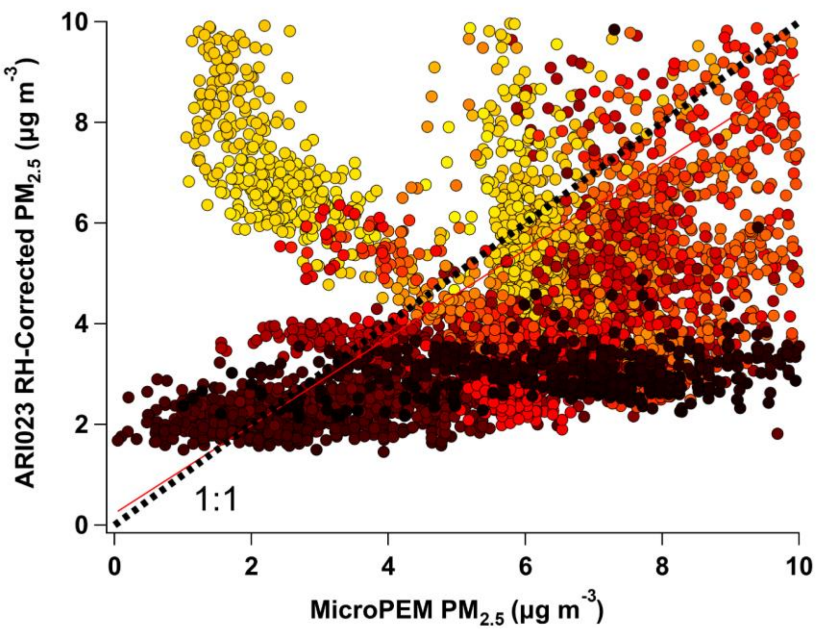

Figure S7: Zoom of Figure S6b.

Table S1: (Top) Metrics from the MicroPEM and OPC-N2 observations (with and without RH-correction) during collocation for three averaging intervals. Metrics for RH-corrected, 1-hr averaged data stratified by ambient concentration (as measured by MicroPEM), RH, and wind direction are given in subsequent tables below.

Averaging Interval	**Slope**	**Intercept**	**R^2**	**MAE**	**Cv**
1 min	1.6	-0.07	0.1	9.0	0.7
1 hr	0.7	8.5	0.03	8.7	0.6
24 hr	-0.9	24	0.2	8.5	0.5
1 min RH Corrected	0.87	0.2	0.2	5.8	0.6
1 hr RH Corrected	0.43	4.3	0.06	5.4	0.6
24 hr RH Corrected	-0.27	11	0.1	4.2	0.5

Concentration ($\mu g\ m^{-3}$)	**Slope**	**Intercept**	**R^2**	**MAE**	**Cv**
0-5	-2.2	14	0.064	4.1	0.33
5-10	1.3	-1.2	0.025	4.7	0.16
10-15	0.5	4.8	0.004	8.5	0.11
15-20	1.3	-11	0.016	9.3	0.04
20-105	0.38	3.1	0.174	16.8	0.36

RH (%)	**Slope**	**Intercept**	**R^2**	**MAE**	**Cv**
10 to 20	0.47	0.5	0.356	6.2	0.67
20 to 30	0.53	0.7	0.725	3.8	0.89
30 to 40	0.45	1.4	0.629	3.7	0.59
40 to 50	0.53	1.6	0.432	4.2	0.53
50 to 60	0.47	2.1	0.379	4.9	0.50
60 to 70	0.61	0.5	0.307	5.2	0.47
70 to 80	0.19	9.7	0.005	7.1	0.60
80 to 90	1.2	8.9	0.025	11	0.37

Wind direction	**Slope**	**Intercept**	**R^2**	**MAE**	**Cv**
N	0.41	2.5	0.125	3.31	0.55
NE	0.57	0.7	0.489	3.83	0.69
E	0.51	5.2	0.057	6.12	0.84
SE	0.41	4.8	0.042	5.80	0.75
S	0.31	5.3	0.042	5.91	0.63
SW	0.45	2.7	0.148	4.09	0.62
W	0.40	2.9	0.267	3.00	0.70
NW	0.62	1.2	0.342	3.38	0.61

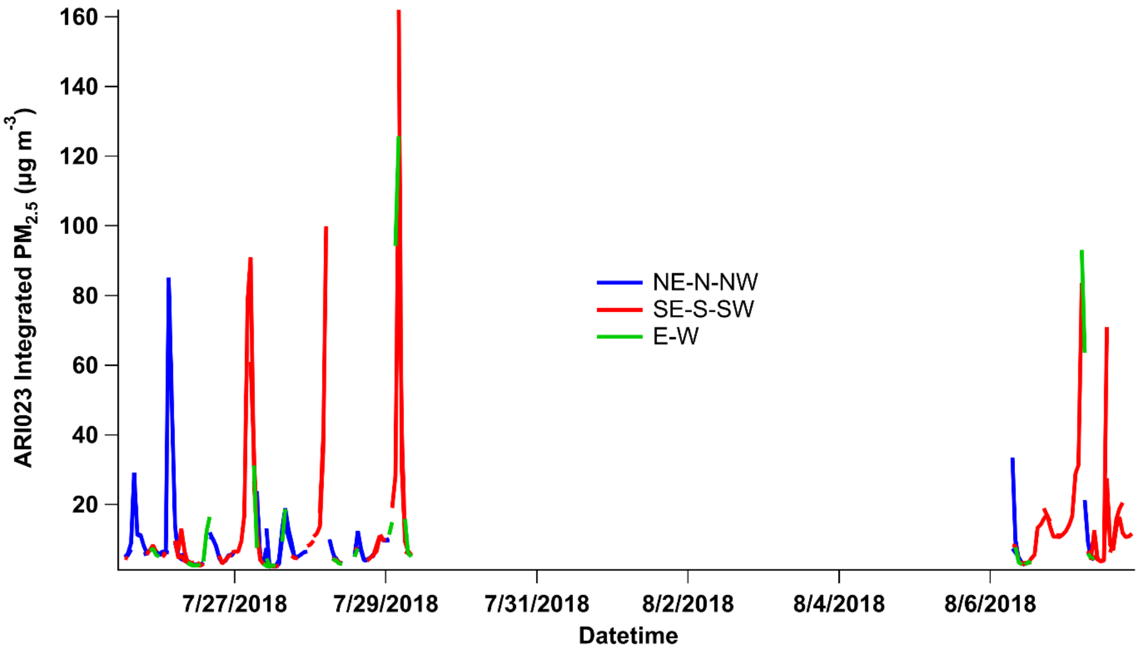

Figure S8: Times series of ARISense 023 un-corrected $PM_{2.5}$ concentration during collocation in Malawi. Spikes in the time series are associated with widespread biomass cookstove use during the morning (5-7 AM). Data are colored by wind direction. Cookstove activity was largely associated with southerly winds.

Table S2*:* Performance metrics of $PM_{2.5}$ mass concentration measurements from the Alphasense OPC-N2 (ARI023) compared to the mass-corrected MicroPEM nephelometer during collocation in Malawi. The number of data points in all three scenarios are identical, but the assumed kappa value, applied as part of an RH-correction algorithm, is different. This RH-correction algorithm is based on the kappa value and 'shifting' the bin cut-offs (Di Antonio, et al. 2018). In this case, the assumed density is held constant, and the kappa value is changed. $\kappa = 0.6$ is the empirical value which achieved the best agreement between an OPC-N2 and reference data in the UK (Di Antonio (2018)). $\kappa = 1$ indicates an aerosol mixture with appreciable amounts of inorganics (theoretical value, based on Petters & Kreidenweis (2007)). $\kappa = 0.15$ was reported to be the continental average value for Africa, based on Pringle et al, 2010 and Pope at. al, 2018 (modelled and observed). Data are 60-min averaged. R^2 = Coefficient of Determination, Cv = Coefficient of Variation, MAE = Mean Absolute Error.

Kappa	**Slope**	**Intercept**	**R^2**	**MAE**	**Cv**
0.15	0.589	5.44	0.051	6.54	0.59
0.6	0.41	4.31	0.068	5.42	0.59
1	0.32	3.57	0.076	5.40	0.59

Table S3: Performance metrics of PM2.5 mass concentration measurements from the Alphasense OPC-N2 (ARI023) compared to the mass-corrected MicroPEM nephelometer during collocation in Malawi. The number of data points in all scenarios are identical, but the assumed kappa value, applied as part of an RH-correction algorithm, and the assumed density is different in each. This RH-correction algorithm is based on the kappa value and 'shifting' the bin cut-offs (Di Antonio, et al. 2018). Species data (κ and density) based on Hagan & Kroll (2020) & Petters & Kreidenweis (2007). Data are 60-min averaged. R^2 = Coefficient of Determination, Cv = Coefficient of Variation, MAE = Mean Absolute Error.

Aerosol source type	Kappa	Density (g cm^{-3})	Slope	Intercept	R^2	MAE	Cv
Ammonium Nitrate	0.67	1.72	0.42	4.17	0.076	5.32	0.59
Dust	0.03	2.6	0.58	5.88	0.044	6.85	0.59
Wildfire	0.1	1.58	1.02	11.8	0.033	12.7	0.59
Background	0.25	1.45	0.35	5.84	0.025	6.69	0.59

S4 Description of assessment metrics

Table S4: EPA recommended performance metrics and target values for low-cost gas (ozone) and particle sensor evaluation. Adapted from Tables ES-2 (Duvall et al., 2021a, b). We use Mean Absolute Error in place of (RMSE).

Performance Metric		**O_3 Target Value**	**$PM_{2.5}$ Target Value**
Precision	Standard deviation (SD) **OR**	≤ 5 ppbv	≤ 5 µg m^{-3}
	Coefficient of Variation (CV)	≤ 30%	≤ 30%
Bias	Slope (m)	1.0 ± 0.2	1.0 ± 0.35
	Intercept (b)	-5 ≤ b ≤ 5 ppbv	-5 ≤ b ≤ 5 µg m-3
Linearity	Coefficient of Determination (R^2)	≥ 0.80	≥ 0.70
Error	Root Mean Square Error (RMSE)	≤ 5 ppbv	RMSE ≤ 7 µg m-3 **or** NRMSE ≤ 30%

The correlation between estimated and true concentrations is assessed using the true predictive correlation coefficient or the "Coefficient of Determination". For *n* measurements,

$$R^2 = 1 - \frac{\sum_{i=1}^{n}\left(c_{true,i} - c_{estimated,i}\right)^2}{\sum_{i=1}^{n}\left(\Delta c_{true,i}\right)^2} \tag{1}$$

where $c_{estimated,i}$ is the measured concentration as measured by the ARISense monitor, $c_{true,i}$ is the corresponding actual concentration as measured by the reference instrument, and

$$\Delta c_{true,i} = c_{true,i} - \frac{1}{n}\sum_{j=1}^{n} c_{true,j} \tag{2}$$

The error in the ARISense measurements compared to the reference measurements is assessed using the mean absolute error (MAE):

$$MAE = \frac{\sum_{i=1}^{n} |c_{estimated,i} - c_{true,i}|}{n} \quad (3)$$

To assess precision:

$$cV = \frac{\sqrt{\frac{\sum_{i=1}^{n} \Delta c_{estimated,i}^{2}}{n}}}{\frac{1}{n}\sum_{j=1}^{n} c_{estimated,j}} \quad (4)$$

where

$$\Delta c_{estimated,i} = c_{estimated,i} - \frac{1}{n}\sum_{j=1}^{n} c_{estimated,j} \quad (5)$$

To assess bias, we fit a linear regression model to compare the slope and intercept:

$$c_{estimated} = m * c_{true,i} + b \quad (6)$$

where m is the slope and b is the y-intercept.

To estimate the interval for the average diurnal OPC-N2 measurements we applied a Box-Cox transformation (Box and Cox, 1964) to the linear regression model:

$$c_{estimated}(\lambda) = (c_{estimated}^{\lambda} - 1)/\lambda \quad (7)$$

with λ = -0.14 to obtain an error term in the linear regression model independent of c_{true} and normally distributed, with zero mean and constant variance. Interval estimates for future OPC-N2 measurements were calculated as prediction intervals:

$$c_{estimated}(\lambda) \pm t_{1-\frac{\alpha}{2}, n-2} \sqrt{\frac{1}{n}\sum_{i=1}^{n}\left(c_{estimated,i} - c_{true,i}\right)^{2} * \left(1 + \frac{1}{n} + \left(\frac{\Delta c_{true}(\lambda))^{2}}{\sum_{i=1}^{n}(\Delta c_{true,i})\text{^}2}\right)\right.} \quad (8)$$

where t is the t-statistic value for a given level of significance α. The prediction intervals were reverse-transformed and used to estimate the range for future to $c_{estimated}$ measurements. The ARI023 MicroPEM measurements were $c_{true,i}$ and OPC-N2 were $c_{estimated}$. Outlying observations occurring between 3-6 AM were excluded for the fit to converge due to high ambient RH conditions (> 75%) coinciding with periods of fresh, biomass emissions from nearby morning cooking activity. The analysis was completed in R (version 3.6.0) using RStudio (version 1.2.5042) with *MASS* (version 7.3-51.4) and *ggplot2* (version 3.3.2) libraries.

To calculate the prediction intervals for ARI013, ARI014, and ARI015, we used collocation data from the ARI023 Alphasense OPC-N2 deployed in 2018 to the Village 2 site in Malawi (Figure S8). We surmise the results from the collocation data of ARI023 can be extrapolated to the 2017 ARI013-ARI015 data set for the following reasons: a) this is the best-available in situ collocation data for our specific deployment conditions and source aerosol, b) we observed highly similar responses from the Alphasense OPC-N2 units in ARI013, ARI014, and ARI015 during collocations (R^2 > 0.9), and c) we only aimed to report low confidence level (1-sigma) prediction intervals with our measurements. There are caveats to this approach; review studies have reported low repeatability and reproducibility across Alphasense OPC-N2 units (Rai et al., 2017), but several studies have reported high inter-unit agreement with a cV around 0.2 (Bulot et al., 2019; Crilley et al., 2018; Badura et al., 2018).

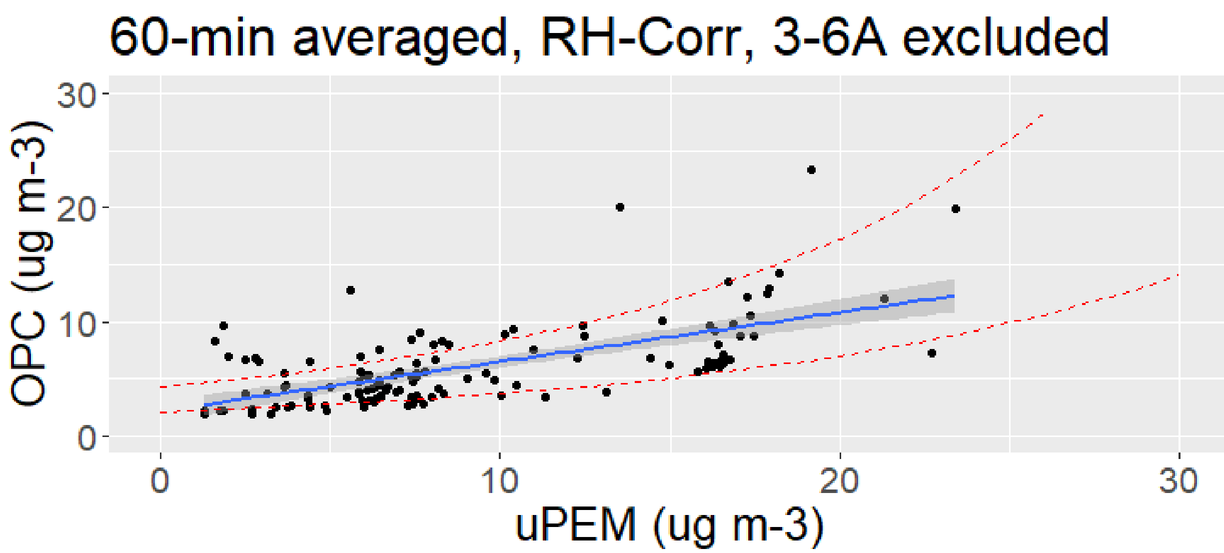

Figure S8: Alphasense OPC-N2 RH-corrected $PM_{2.5}$ mass concentration versus MicroPEM $PM_{2.5}$ concentration data used for the linear model; Fit line shown in blue, grey shaded area indicating 68% confidence interval in slope; Dotted red lines indicate 68% prediction interval upper and lower limits calculated from the linear model. Data are 60-min averaged. Data collected from 3-6 AM (morning cooking periods) were removed for the fit to converge.

(a)

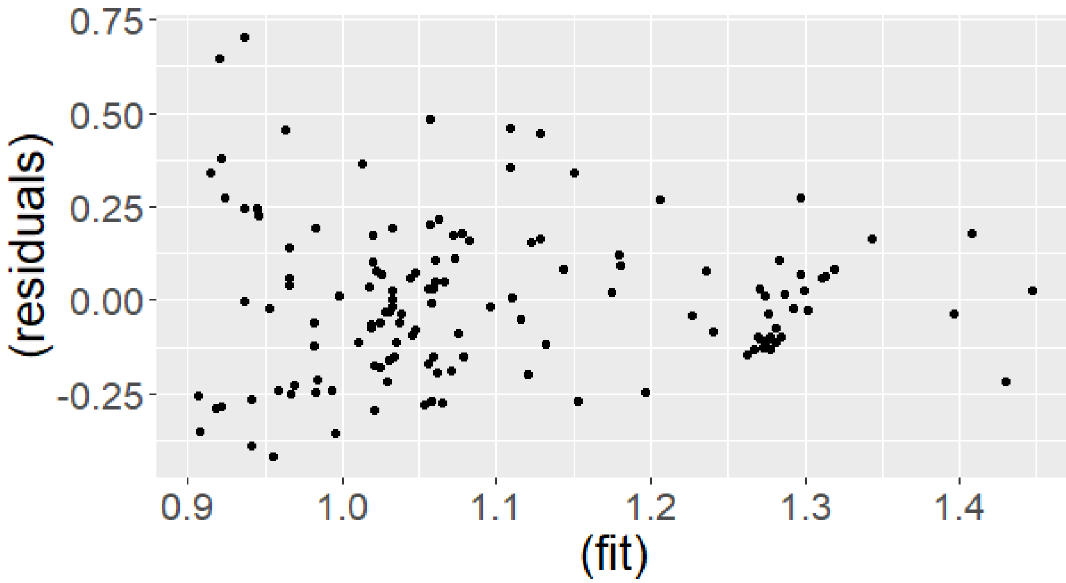

(b)

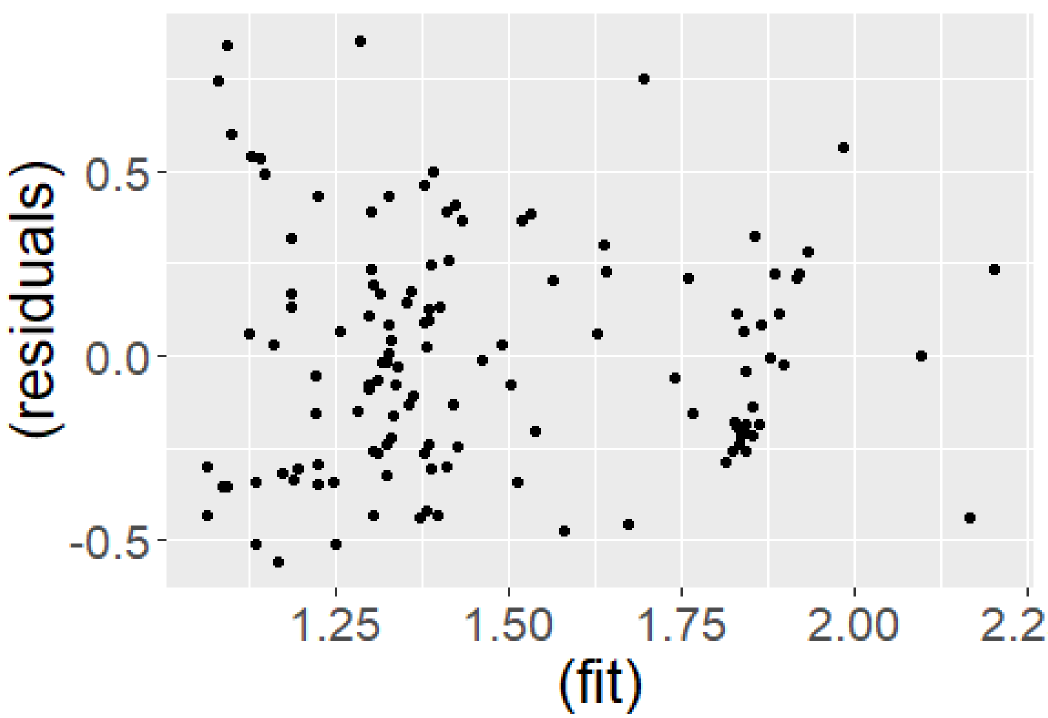

Figure S9: RH-corrected OPC-N2 $PM_{2.5}$ mass concentration (1-hr averaged) linear model residuals and fit range. Residuals = difference between OPC-N2 and MicroPEM measurements; (a) raw data, and (b) box-cox transformed data with outliers occurring from 3-6 AM LT (the morning cooking period) excluded.

S5 Details of Malawi Deployments

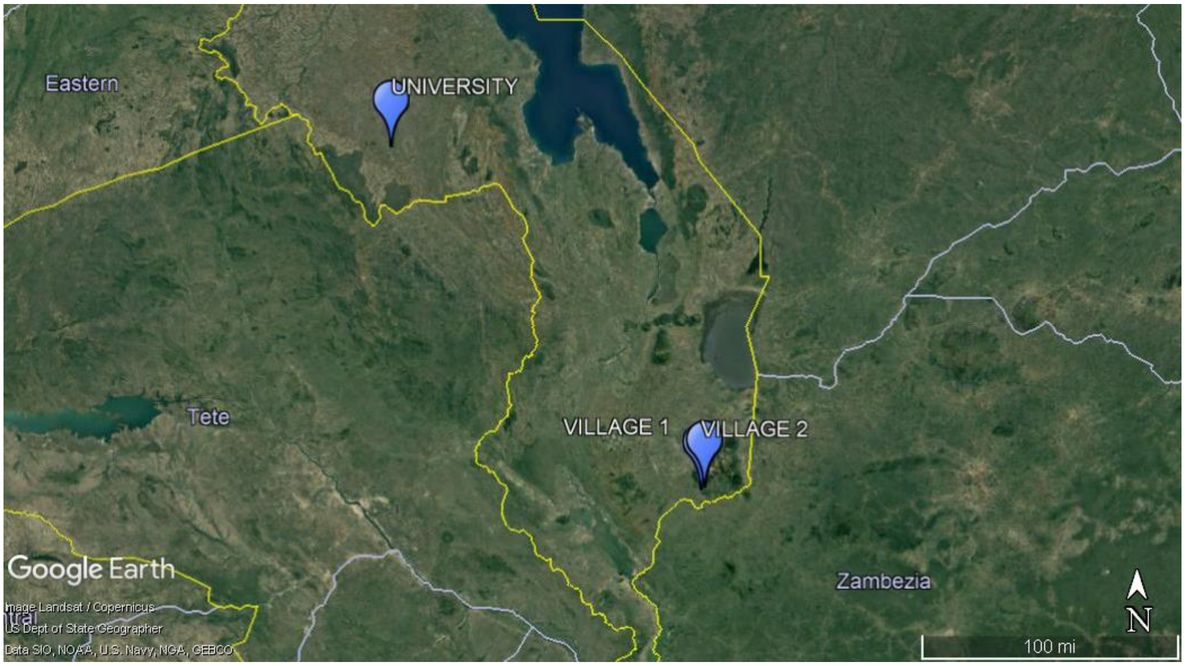

Figure S10: Satellite map of Malawi, blue markers indicate ARISense monitoring sites. Image source: © Google Earth 2020. Google Earth Pro Version 7.3.4.8248. *University, Village 1, and Village 2, Malawi, Southeastern Africa*. Borders and labels layer. Accessed: June 5, 2020.

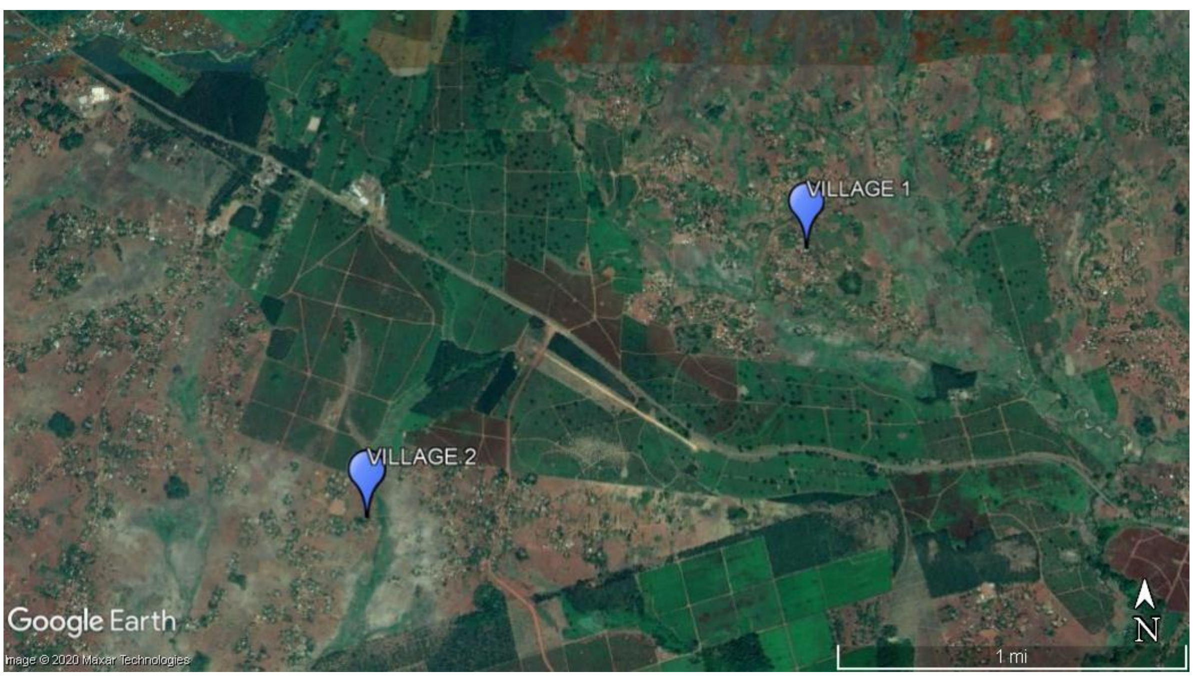

Figure S11: Satellite image of Mulanje "Village" sites, blue markers indicate ARISense monitoring sites. Image source: © Google Earth 2020. Google Earth Pro Version 7.3.4.8248. *Mulanje, Malawi.* Borders and labels layer. Accessed: June 5, 2020.

Figure S12: Satellite image of Village 2 (1000ft scale), blue markers indicate ARISense monitoring sites (ARI013). ARI013 was deployed to the Village 2 site and was mounted on the roof of the residence of the village chief (4 m above ground) in the Mikundi village of Mulanje, Malawi for 382 days from 6 July 2017 to 23 July 2018. Image source: © Google Earth 2020. Google Earth Pro Version 7.3.4.8248. *Mikundi village, Mulanje, Malawi.* 36.056°S, 35.535°E, eye elevation 626 m. Borders and labels layer. Accessed: June 5, 2020.

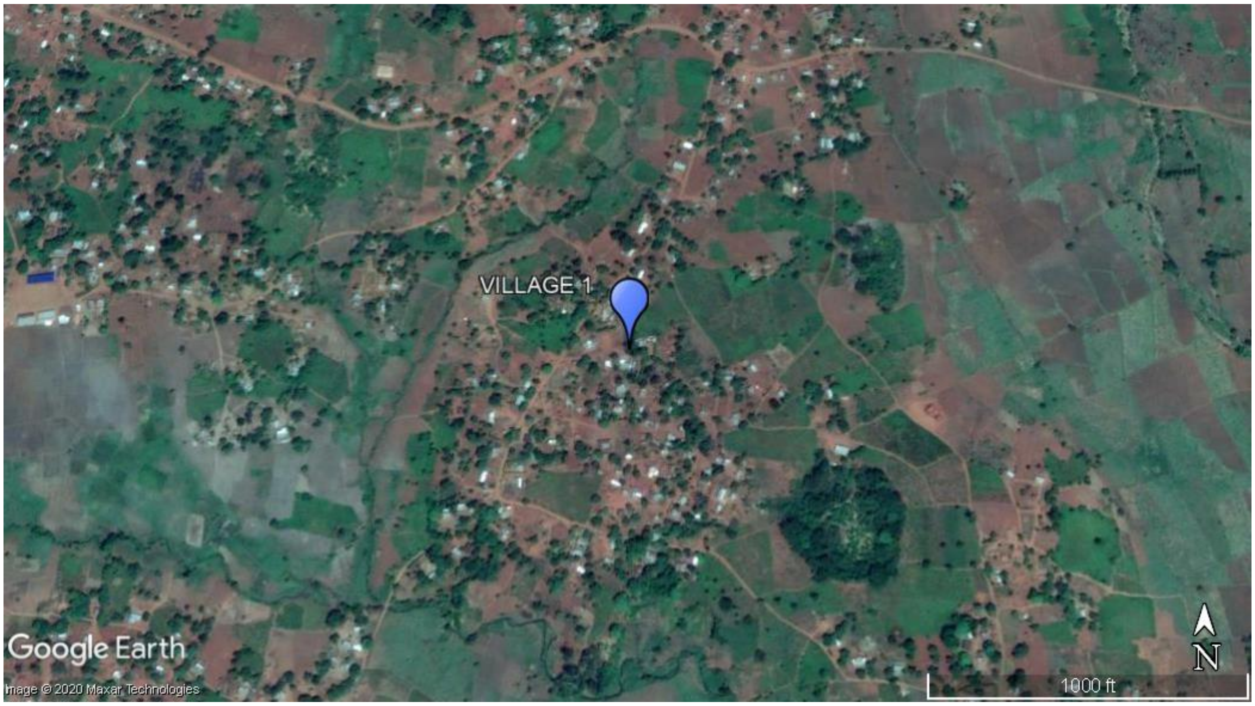

Figure S13: Satellite image of "Village 1" (1000ft scale); blue markers indicate ARISense monitoring sites (ARI014). ARI014 was deployed to Village 1 site and was mounted on the roof of the residence of the village chief (4 m above ground) in the Makaula village of Mulanje, Malawi for 384 days from 11 July 2018 to 30 July 2018. Image source: © Google Earth 2020. Google Earth Pro Version 7.3.4.8248. *Makaula village, Mulanje, Malawi.* 16.045°S, 35.555°E, eye elevation 645 m. Borders and labels layer. Accessed: June 5, 2020.

Figure S14: Satellite image of "University" (1000ft scale), blue markers indicate low-cost monitoring sites (ARI015). ARI015 was deployed to the University site and was mounted on the roof of an office building (7 m above ground) at the Bunda College of Agriculture in the Lilongwe University of Agricultural and Natural Resources near Lilongwe, Malawi for 382 days from 25 June 2017 to 13 July 2018. Image source: © Google Earth 2020. Google Earth Pro Version 7.3.4.8248. *Centre for Agricultural Research, Lilongwe University of Agriculture and Natural Resources, Bunda, Malawi.* 14.180°S, 33.774°E, eye elevation 1125 m. Borders and labels layer. Accessed: June 5, 2020.

(a)

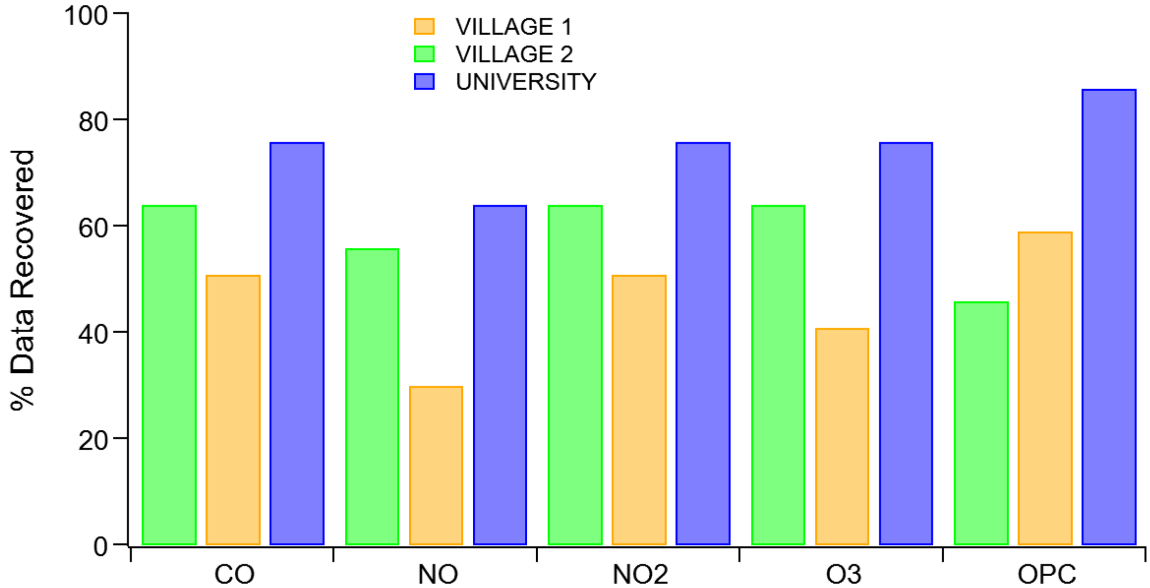

(b)

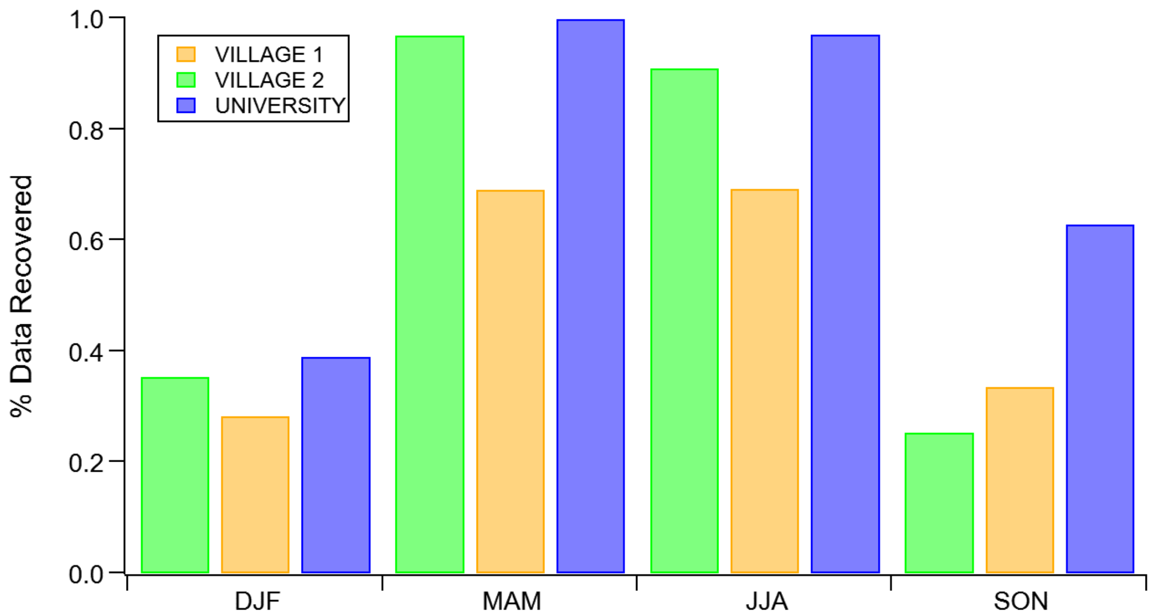

Figure S15: Data recovery rate (%) for the 1-year deployment for each ARISense monitor at their respective sites; (a) shows data recovery by sensor type where CO = carbon monoxide, NO = nitric oxide, NO2 = nitrogen dioxide, O3 = ozone, and OPC = Optical Particle Counter, (b) shows data recovery by season (using the Temperature sensor data recovery rate) where DJF = December-January-February, MAM = March-April-May, JJA = June-July-August, and SON = September-October-November.

S6 Details of remote sensing data

MOPITT and MERRA-2 data were obtained for the Village and University sites. The ARI015 data (University) was located far enough away and was dissimilar enough from the “Villages” data to be kept separate (Fig. S18).

Table S5: NASA Giovanni information used to obtain MOPITT observations for two locations in Malawi.

	Data product	**Spatial Resolution**	**Temporal Resolution**	**Date Range**
MOPITT (satellite observation): The Measurement of Pollution in the Troposphere (MOPITT) sensor launched aboard Terra satellite	Time Series, Area-Averaged of Multispectral CO Surface Mixing Ratio (Daytime/Descending) monthly ()	1°	Monthly	2017-07-01 to 2018-07-31

	User Bounding Box ("Villages")	**User Bounding Box ("University")**	**Data Bounding Box ("Villages")**	**Data Bounding Box ("University")**
	35.5555°, -16.0451°, 35.5555°, -16.0451°	33.7744°, -14.18°, 33.7744°, -14.18°	36°, -16°, 36°, -16°	34°, -14°, 34°, -14°

Table S6: NASA Giovanni information used to obtain MERRA-2 observations for two locations in Malawi.

	Data product	**Spatial Resolution**	**Temporal Resolution**	**Date Range**
MERRA-2 (global atmospheric reanalysis): The Modern-Era Retrospective analysis for Research and Applications, Version 2 (MERRA-2); MERRA-2 Model M2TMNXCHM v5.12.4	Time Series, Area-Averaged of CO Surface Concentration (ENSEMBLE) monthly 0.5 x 0.625 deg. [MERRA-2 ()]	0.5° x 0.625°	Monthly	2017-07-01 to 2018-07-31

	User Bounding Box ("Villages")	**User Bounding Box ("University")**	**Data Bounding Box ("Villages")**	**Data Bounding Box ("University")**
	35.5555°, -16.0451°, 35.5555°, -16.0451°	33.7744°, -14.18°, 33.7744°, -14.18°	35.625°, -16°, 35.625°, -16°	33.75°, -14°, 33.75°, -14°

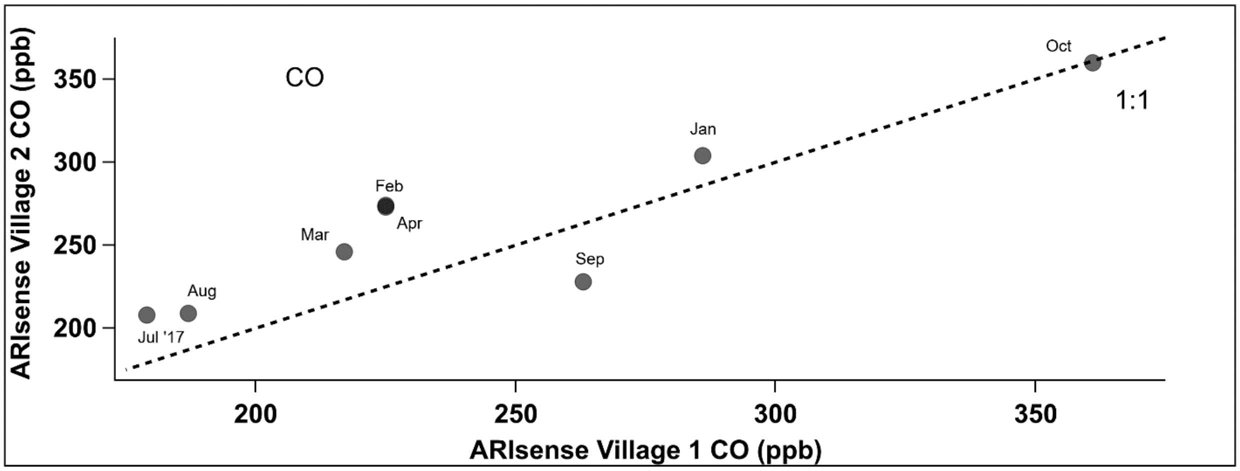

Figure S16: Scatter plot of Village 2 (y-axis) and Village 1 (x-axis) monthly mean CO concentration (calibrated with the kNN Hybrid model). A one-to-one line is shown as the dotted black line.

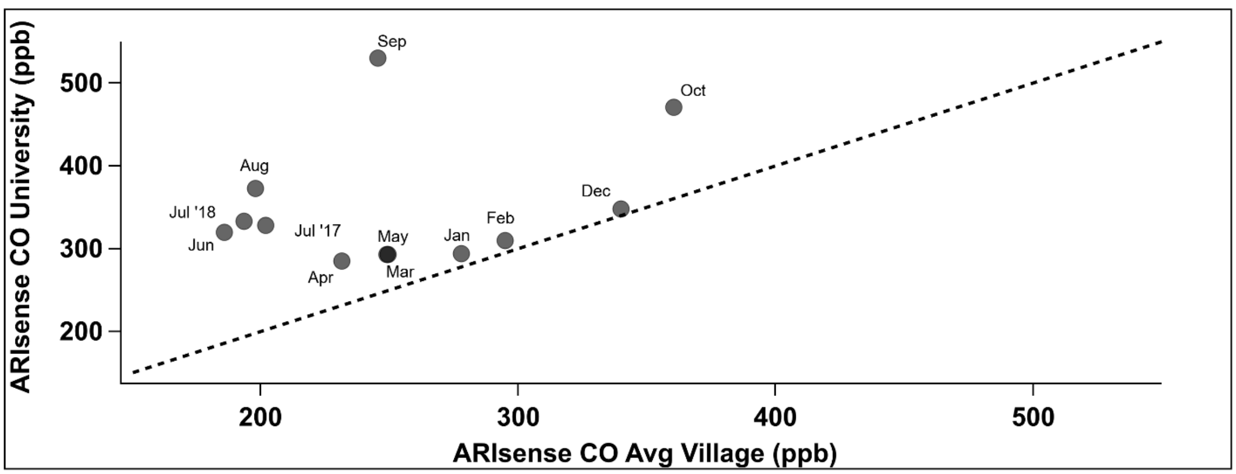

Figure S17: Scatter plot of University (y-axis) and Village (average from Village 1 and 2) (x-axis) monthly mean CO concentration (calibrated with the kNN Hybrid model). A one-to-one line is shown as the dotted black line.

S7 Comparison of NC collocation and Malawi deployment

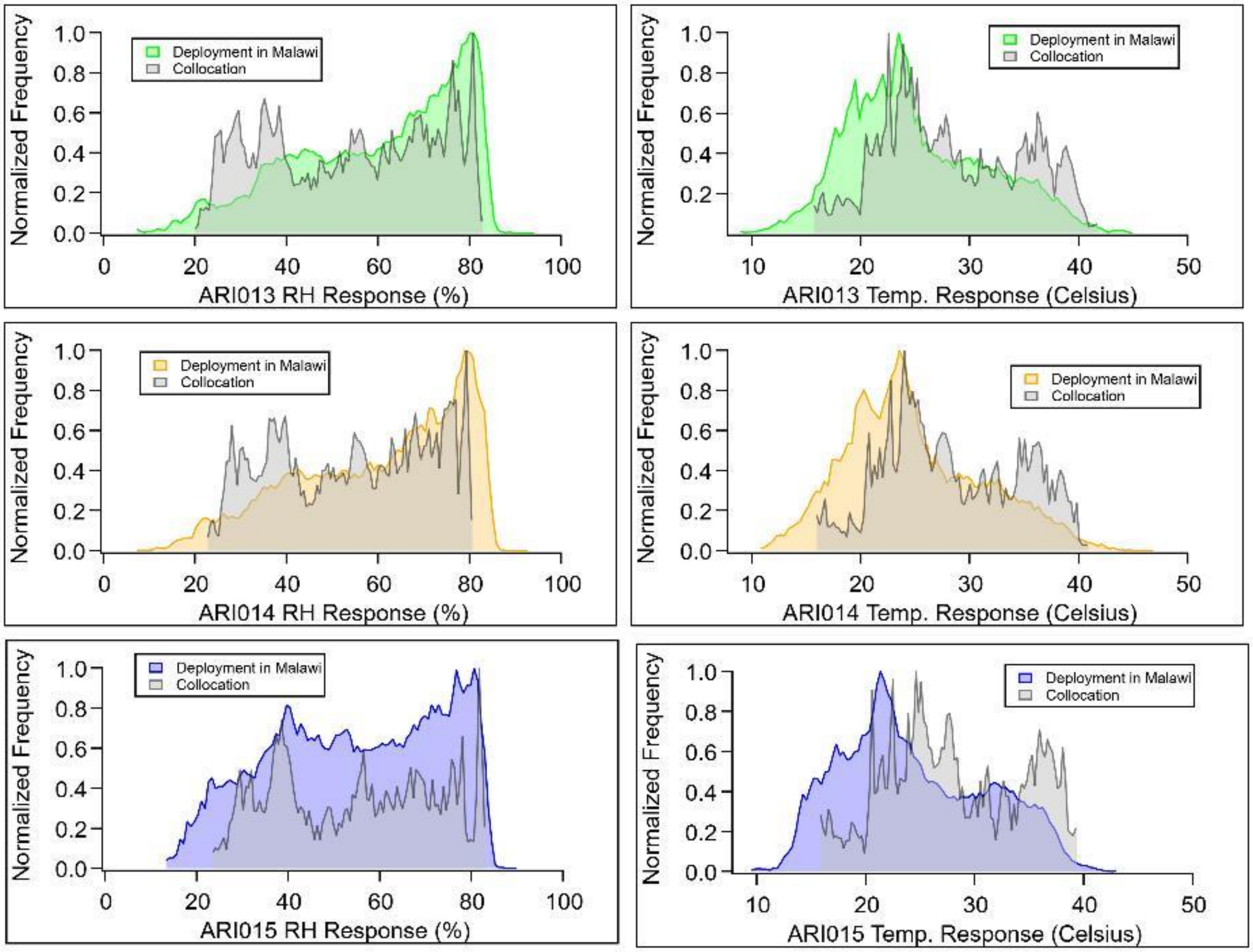

Figure S18: RH (left) and Temperature (right) normalized frequency histograms for the collocation (grey) and deployment (color) environments for all three ARISense monitors. Histogram color indicates ARISense unit number in deployment environment.

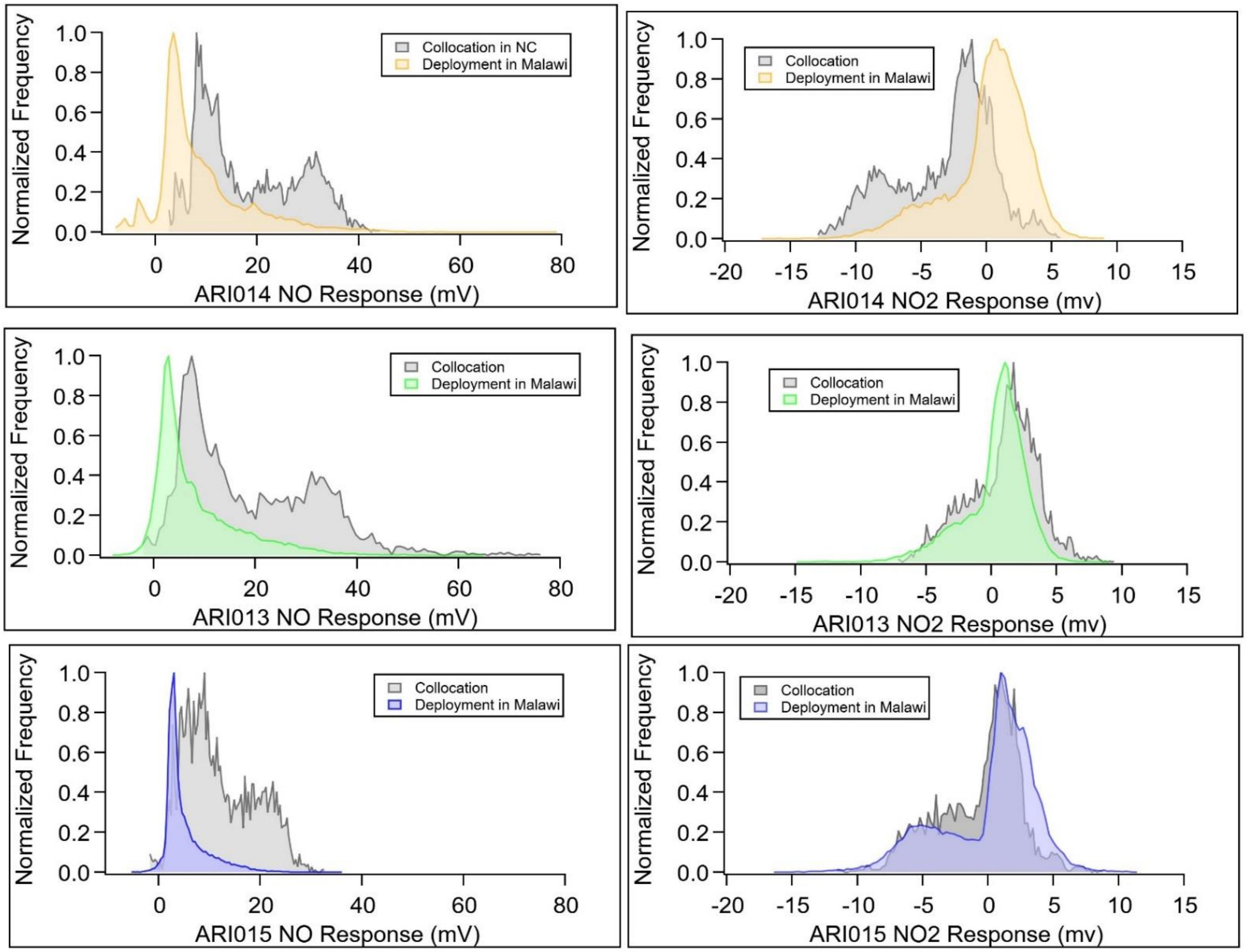

Figure S19: NO (left) and NO2 differential voltage (right) normalized frequency histograms for the collocation (grey) and deployment (color) environments for all three ARISense monitors. Histogram color indicates ARISense unit number in deployment environment.

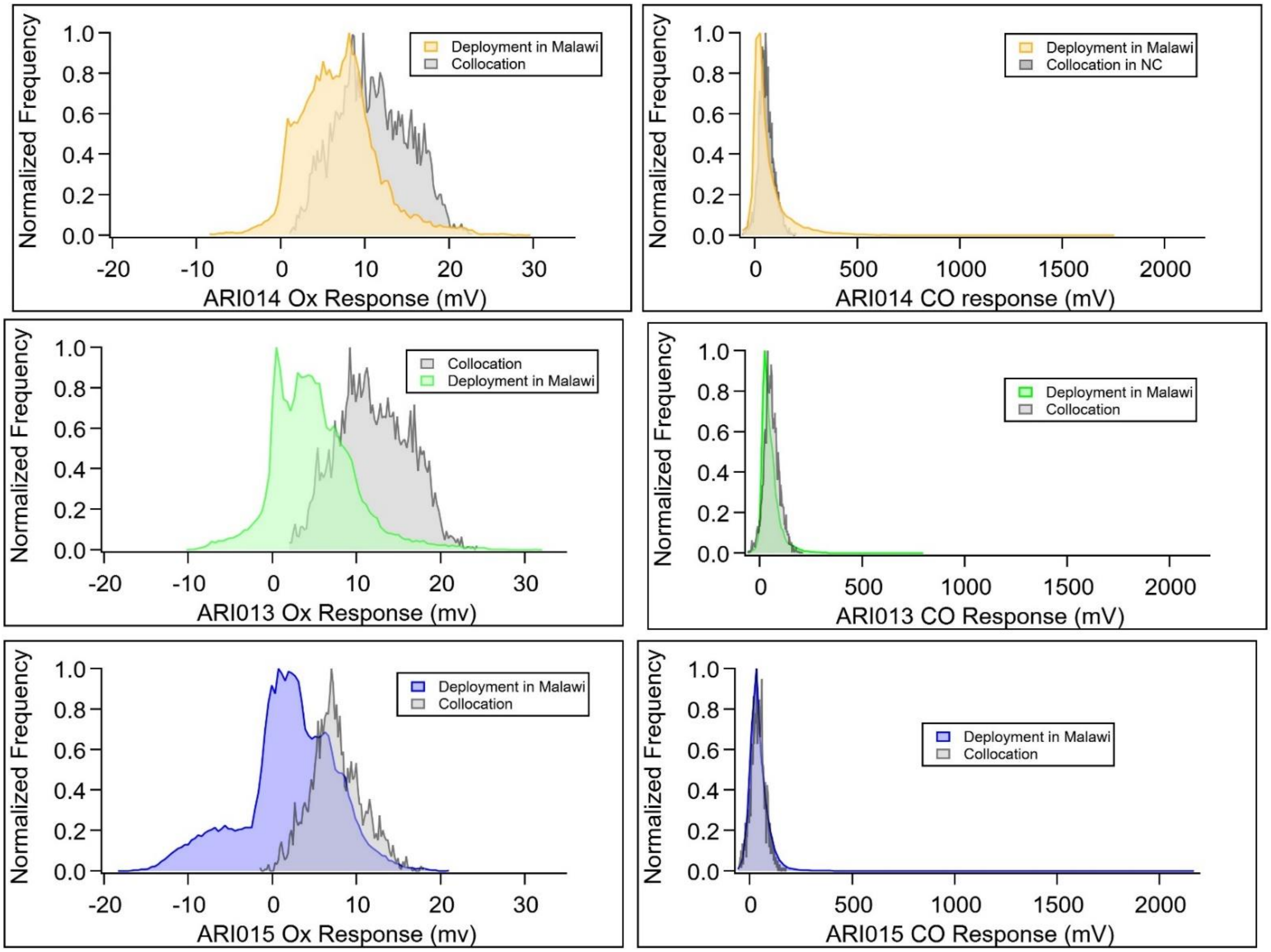

Figure S20: Ox (left) and CO (right) differential voltage normalized frequency histograms for the collocation (grey) and deployment (color) environments for all three ARISense monitors. Histogram color indicates ARISense unit number in deployment environment.

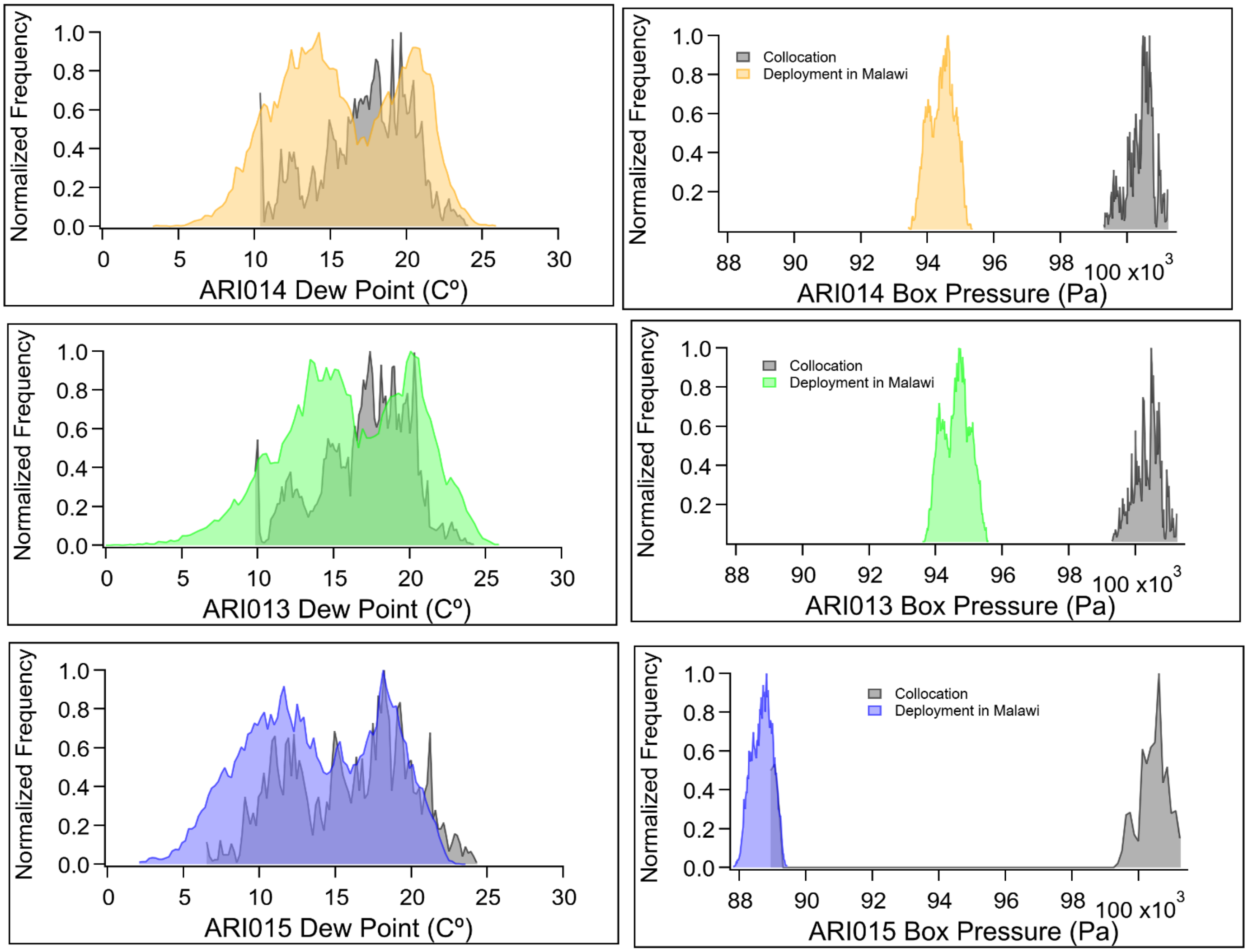

Figure S21: Dew point (left) and pressure (right) normalized frequency histograms for the collocation (grey) and deployment (color) environments for all three ARISense monitors. Histogram color indicates ARISense unit number in deployment environment.

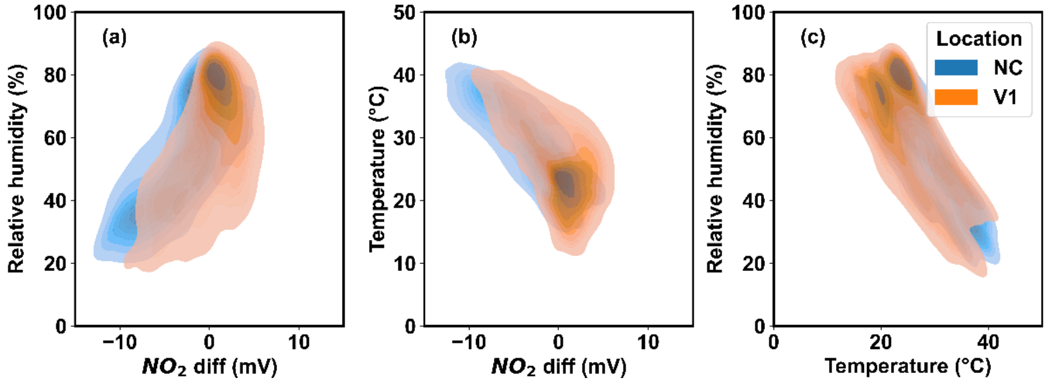

Figure S22: Bivariate distributions of ARI014 NO_2 differential voltage, RH, and T data collected during collocation (blue) and deployment (orange) made using kernel density estimation. NC = North Carolina, V1 = Village 1.

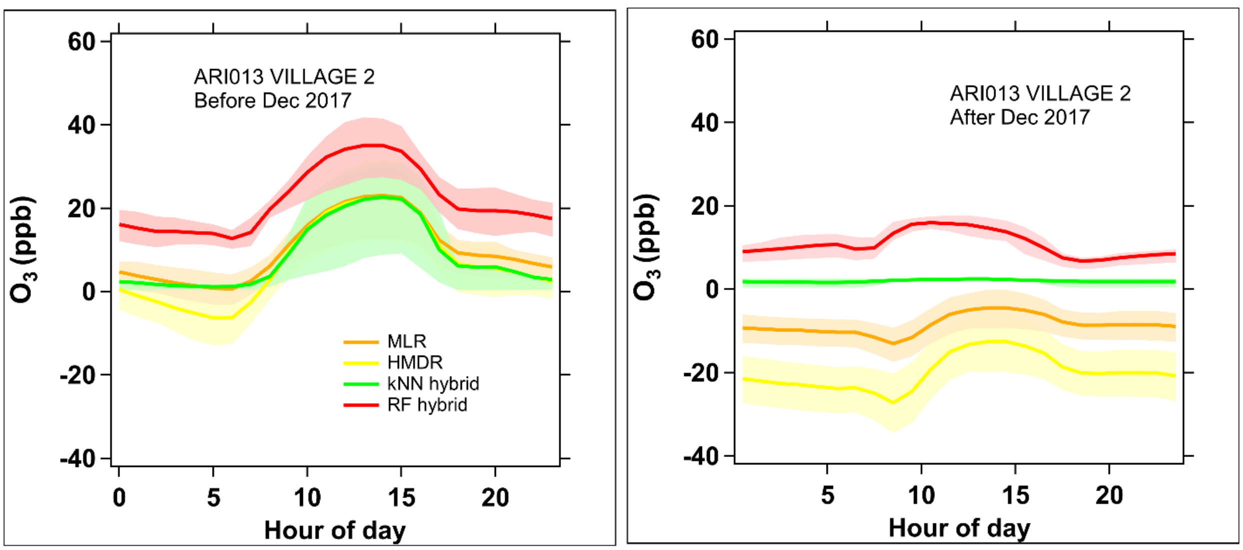

Figure S23*:* Diurnal trends of calibrated ozone data from ARI013 (Village 2 site) before Dec 2017 (left) and after Dec 2018 (right). Thick line indicates hourly mean, shaded region indicates interquartile range. Midnight is the zero hour. Line color indicates model type. Hours are in local time.

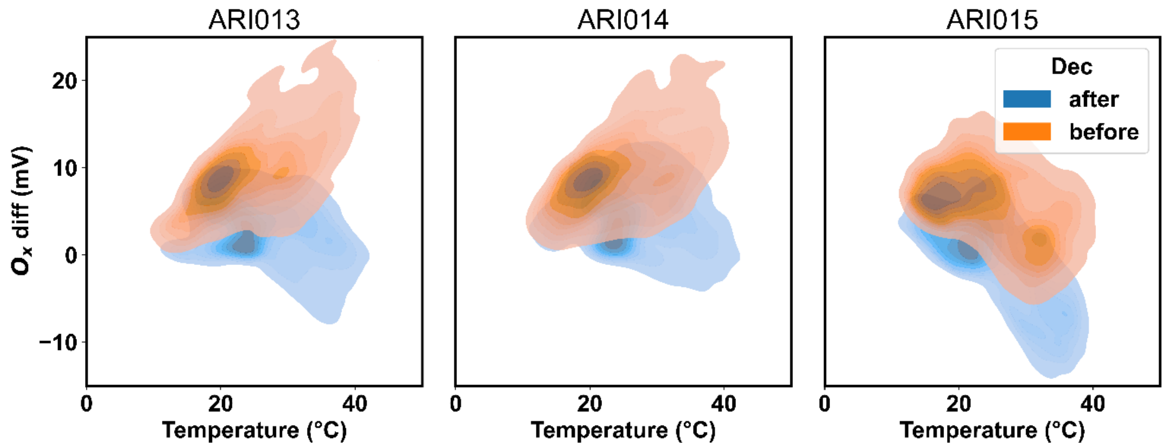

Figure S24: Bivariate distributions of O_x voltage and temperature data collected during the first half of deployment (July-November 2017 - orange) and in the second half of deployment (December 2017-July 2018 – blue) for each ARISense monitor using kernel density estimation.

S8 Comparison of OPC-N2 collocation and deployment in Malawi

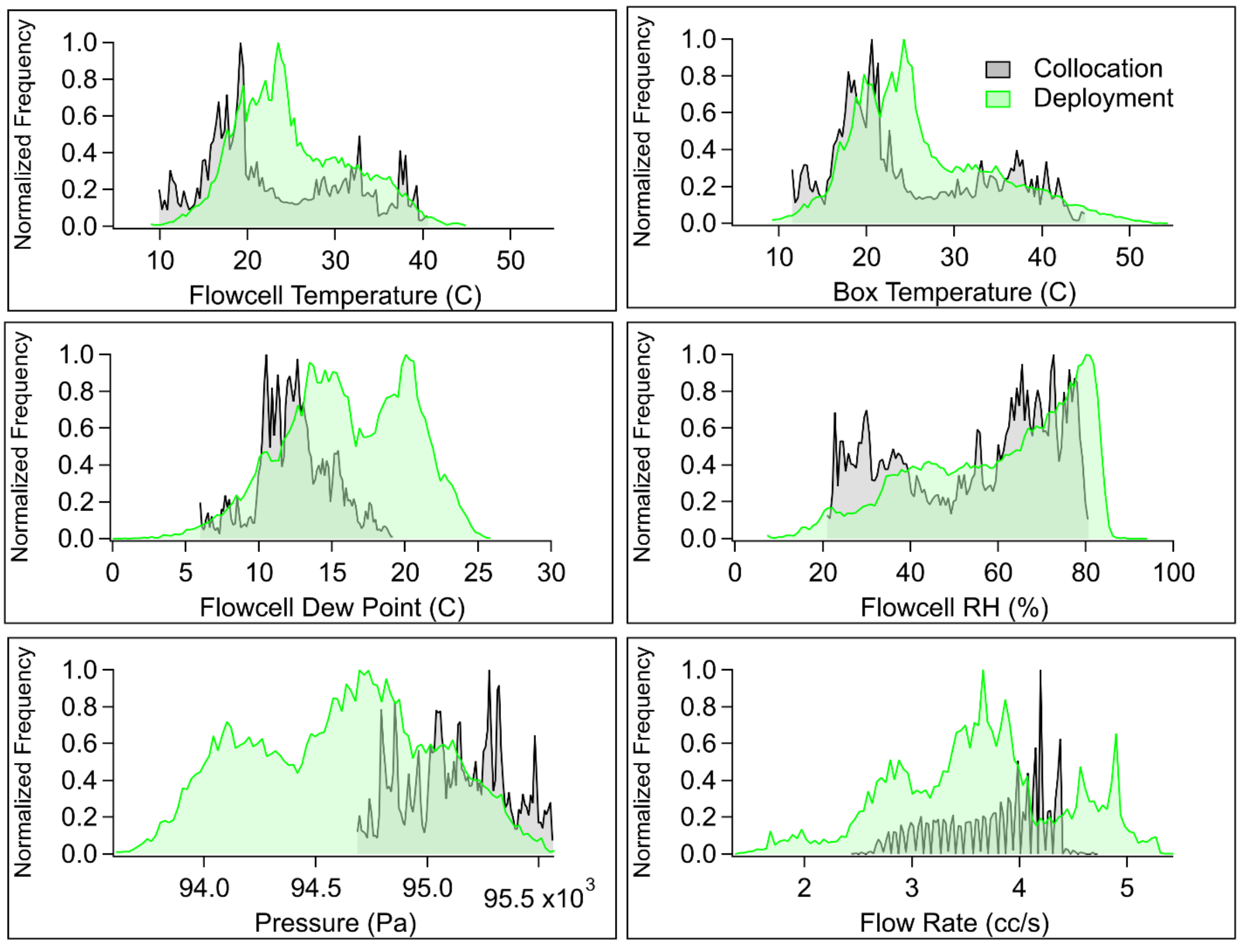

Figure S25: ARISense temperature (flow cell and box), dew point, relative humidity, pressure and flow rate normalized frequency histograms for the 130-hour ARI023 OPC-N2 collocation (grey) in Malawi and the 1-year deployment in Malawi (ARI013 in green.)

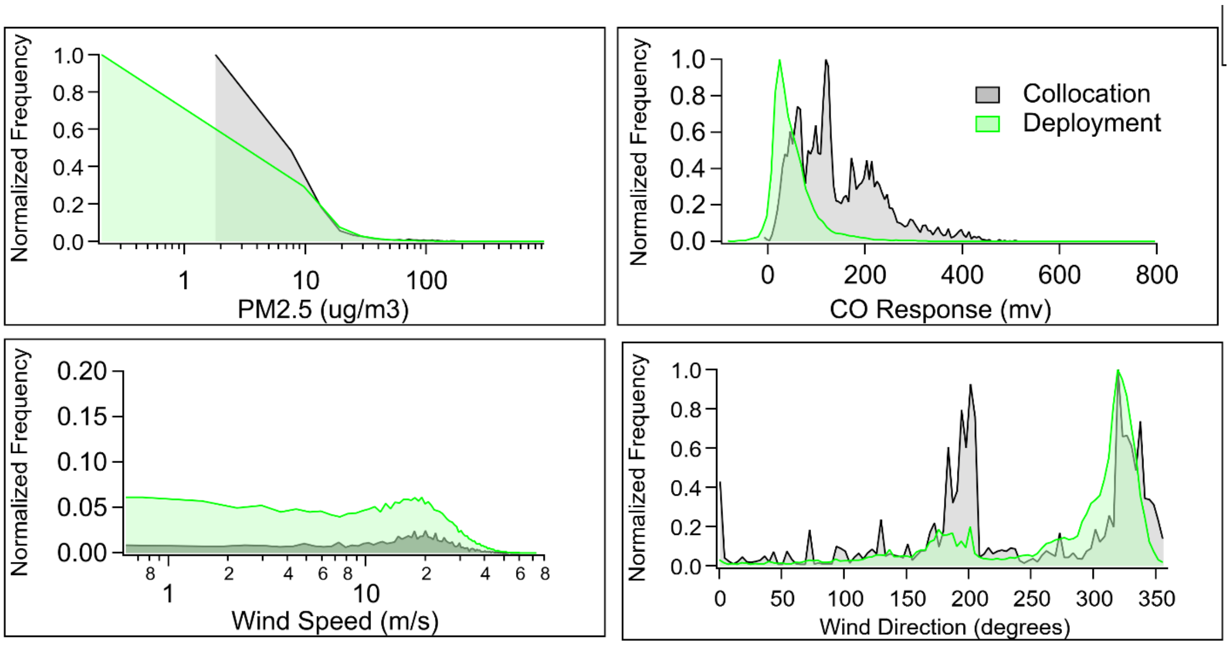

Figure S26: CO differential voltage, $PM_{2.5}$ mass concentration, wind speed, and wind direction normalized frequency histograms for the 130-hour OPC-N2 collocation (ARI023 in grey) in Malawi and the 1-year deployment in Malawi (ARI013 in green).

S9 Comparison of first and last month of deployment data

Histograms of T and RH from July 2017 and July 2018 suggest the range in conditions was the same for both years, particularly for temperature (Fig. S28). However, for the Village 2 site, the average and maximum RH were higher by 10-15% in July 2018 compared to July 2017. Further, the mean temperature was 2° cooler in 2018. Conversely, at the University site in 2018, the average RH was 6% higher, while the minimum RH was 5% lower, compared to 2017 suggesting more variable environmental conditions in the second year. However, for the Village 1 and University sites, the mean temperatures were identical for both years.

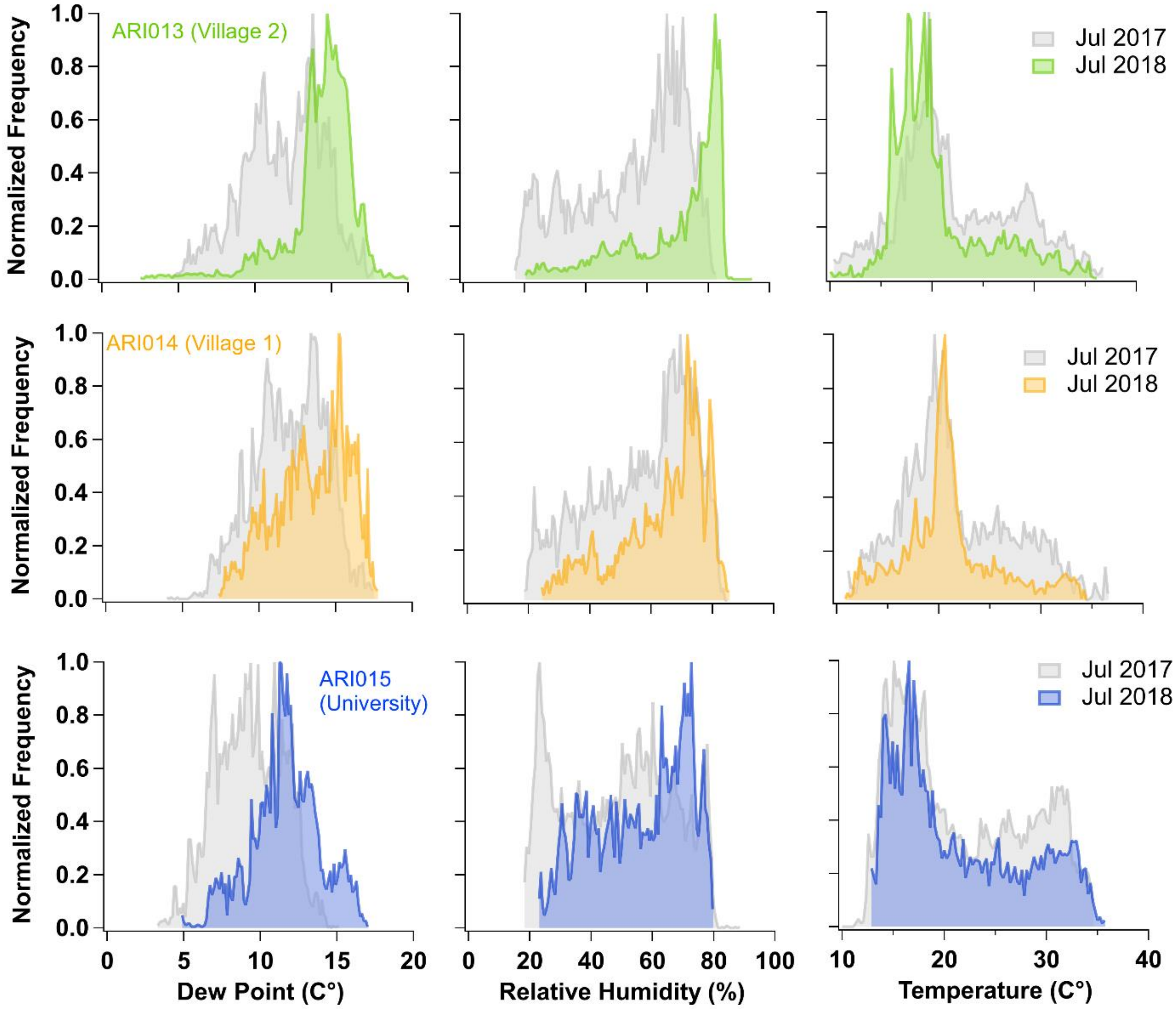

Figure S27: Dew point (left), RH (center), and temperature (right) normalized frequency histograms from the first month of deployment (grey) and last month of deployment (colored) for ARI013, ARI014, and ARI015 at their respective deployment sites.

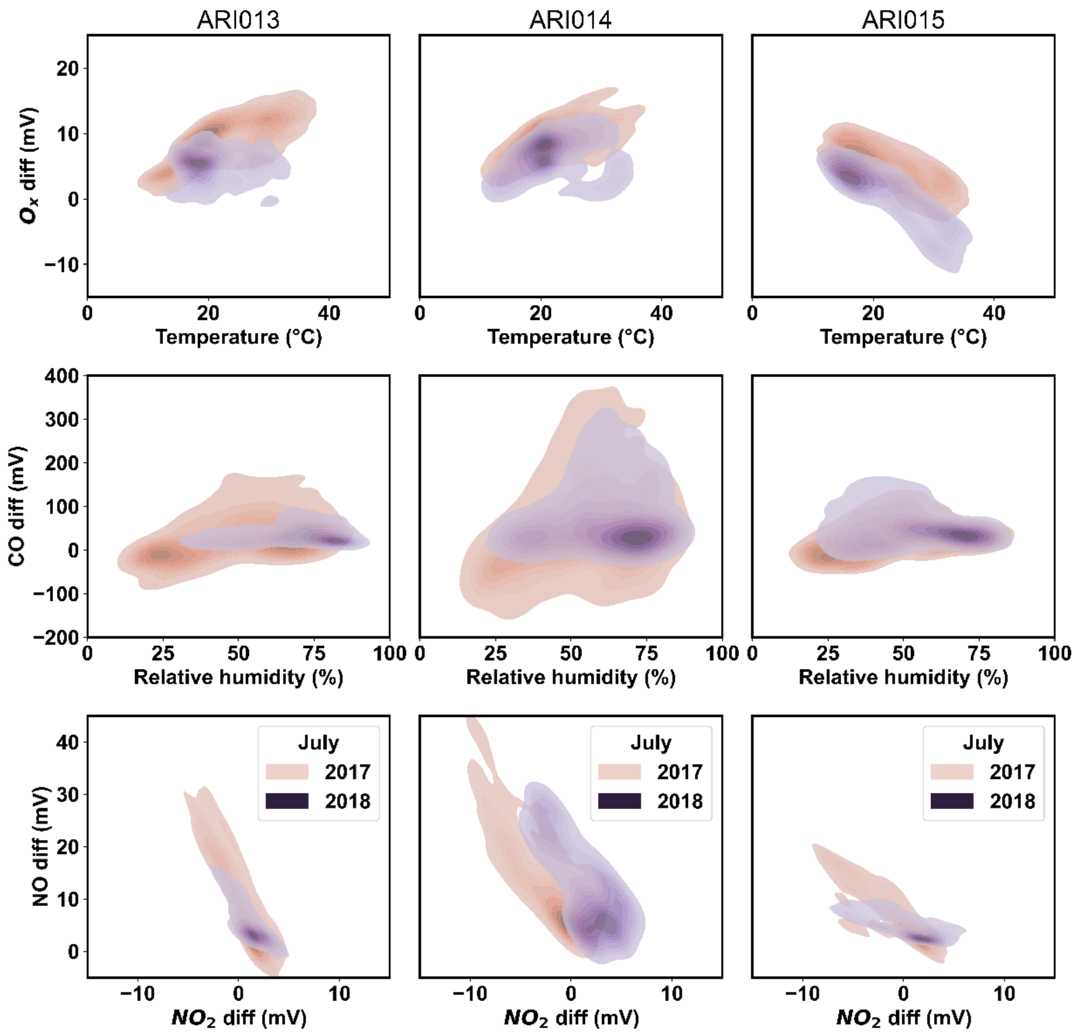

Figure S28: Bivariate distributions of data collected during the first month of deployment (July 2017) and data collected one year later in the last month of deployment (July 2018) for each ARISense monitor using kernel density estimation.

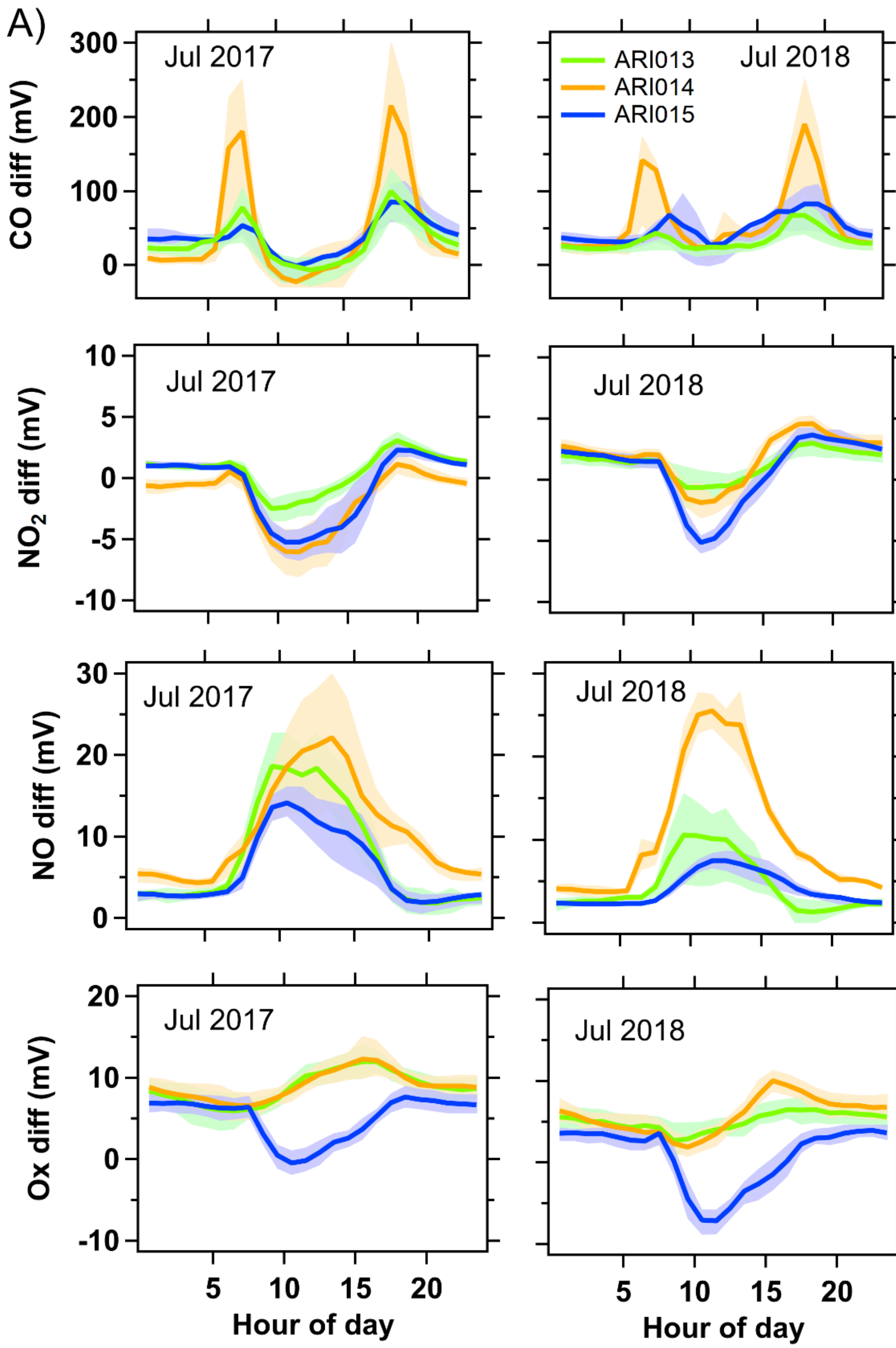

Figure S29*:* Diurnal trends of raw, uncalibrated voltage readings from July 2017 (left) and July 2018 (right), for each ARISense at each respective monitoring location. Thick line indicates hourly mean, shaded region indicates interquartile range. Midnight is the zero hour. Line color indicates sensor.

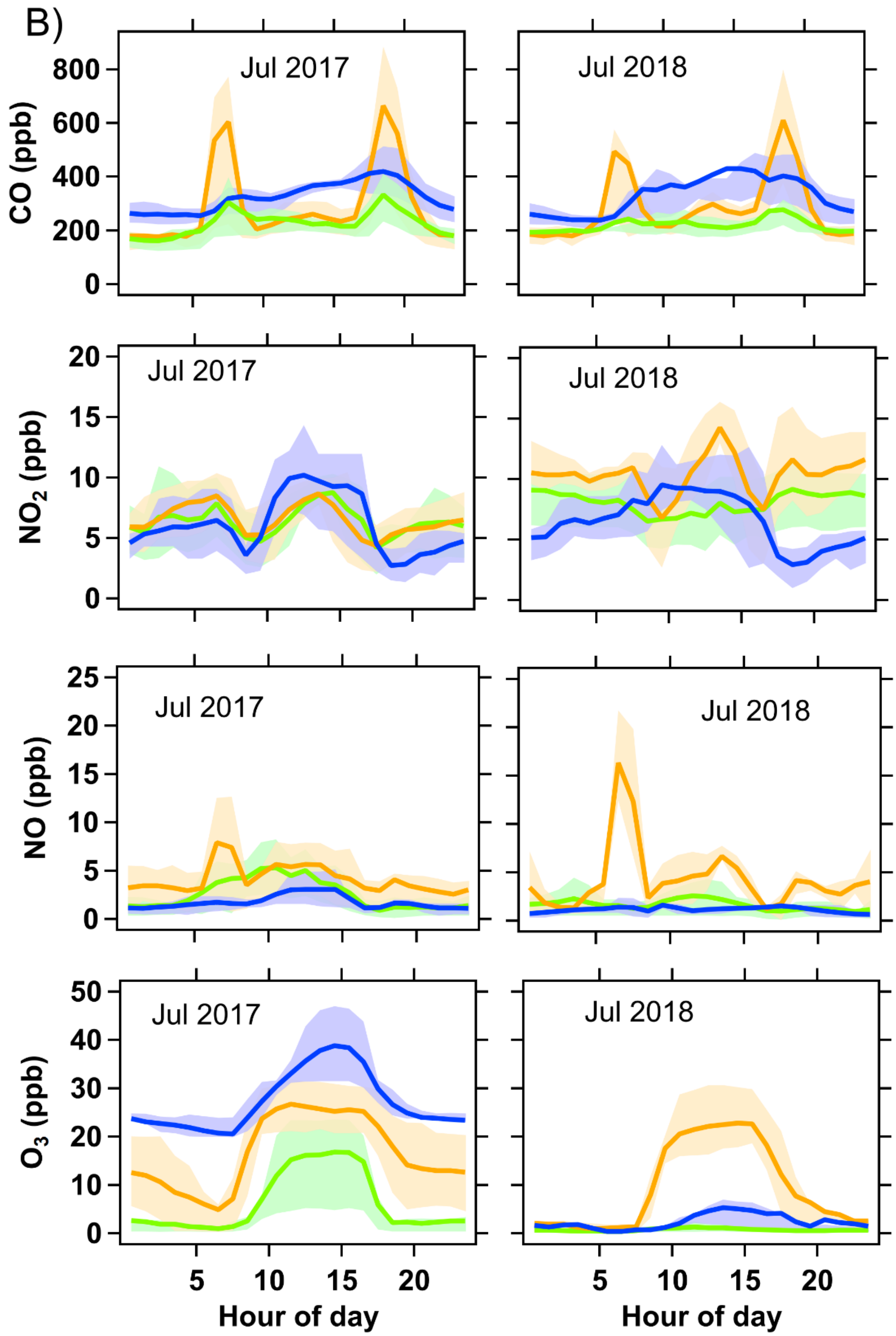

Figure S30: Diurnal trends of kNN-hybrid model calibrated concentration readings from July 2017 (left) and July 2018 (right), for each ARISense at each respective monitoring location. Thick line indicates hourly mean, shaded region indicates interquartile range. Midnight is the zero hour. Line color indicates sensor.

S10 Details of high-concentration biomass burning emission experiments

Emissions measurement equipment, described in Champion and Grieshop (2019), placed near the source measured mean CO concentrations of 50-300 ppb and maximum CO concentrations of 200-3800 ppm. The ARISense were placed further away (3-8 m) from the source. CO sensors saturated (at 5 ppm) for much of the testing period. Depending on the source type, these experiments ranged from 20-48 hours. ARI013 was used for 3 experiments (75 hours total) and ARI014 was used for 4 experiments (100 hours total).

S11 Details of Post-Deployment Collocation in North Carolina

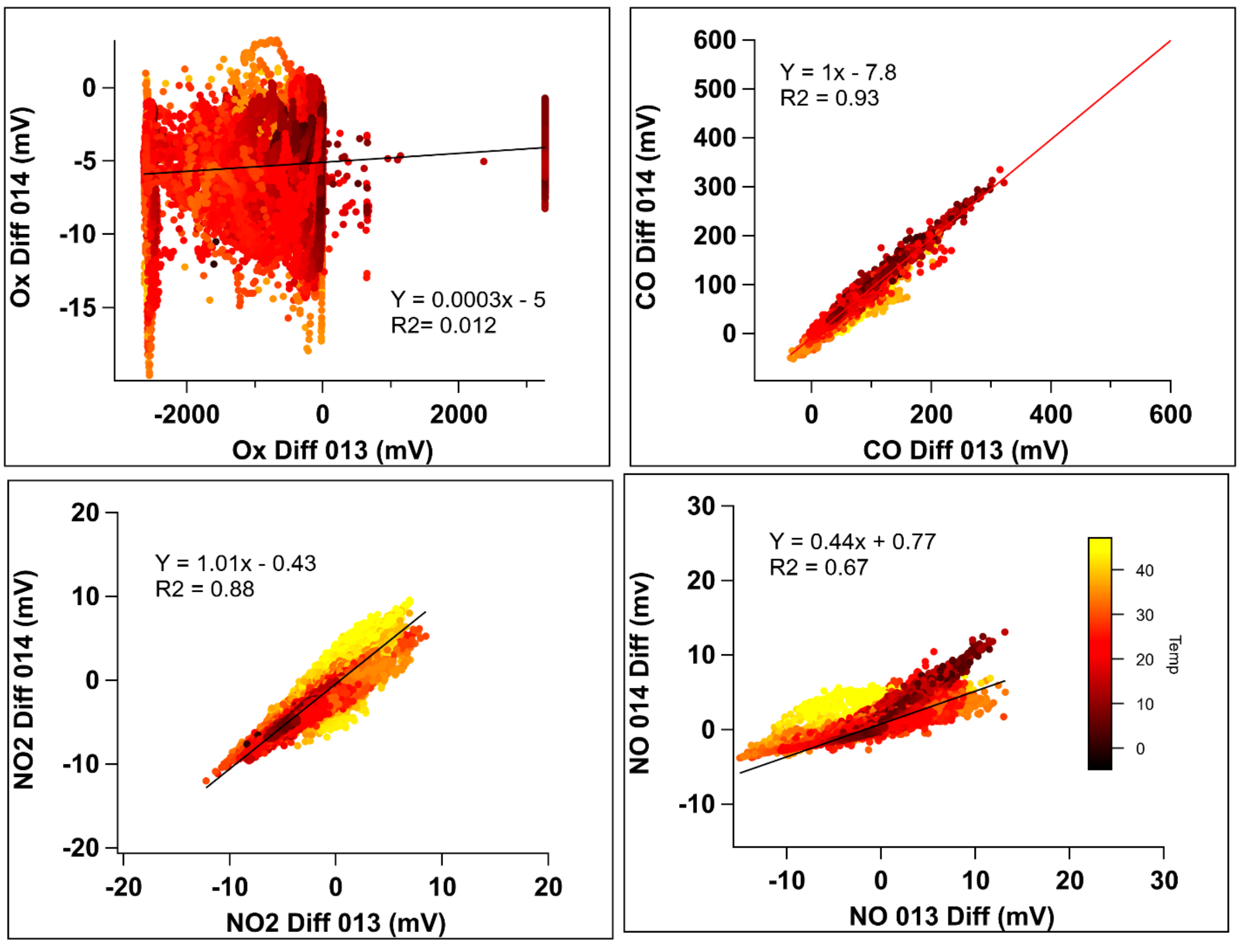

Figure S31: Scatter plots of raw differential voltage data from each gas sensor in ARI014 (y-axis) and ARI013 (x-axis) measured during post-collocation in North Carolina. Linear fit coefficients and Pearson correlation coefficients are shown for each monitor-monitor gas sensor pair. Data points are colored by ambient temperature.

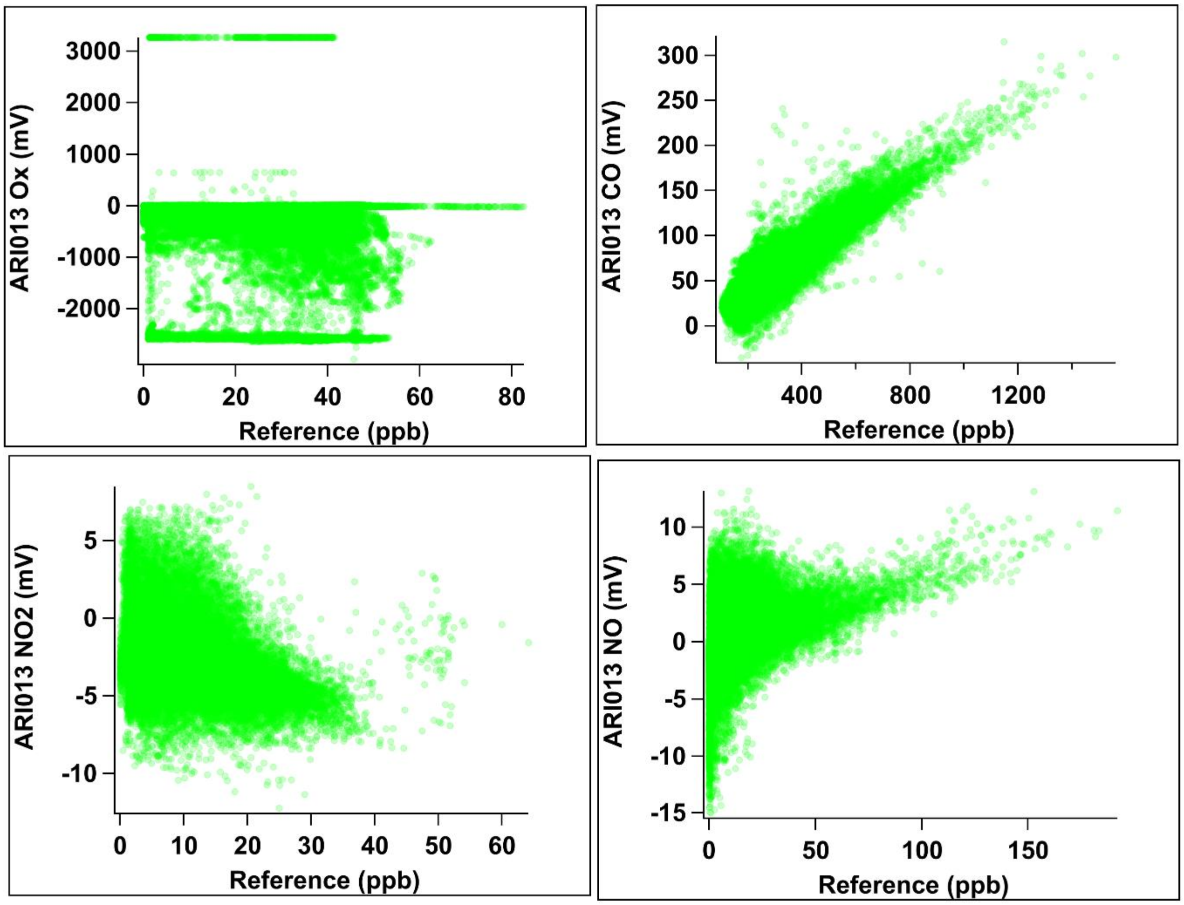

Figure S32: Scatter plots of raw differential voltage data from each gas sensor in ARI013 (y-axis) compared to reference data (x-axis) during post-deployment collocation in North Carolina.

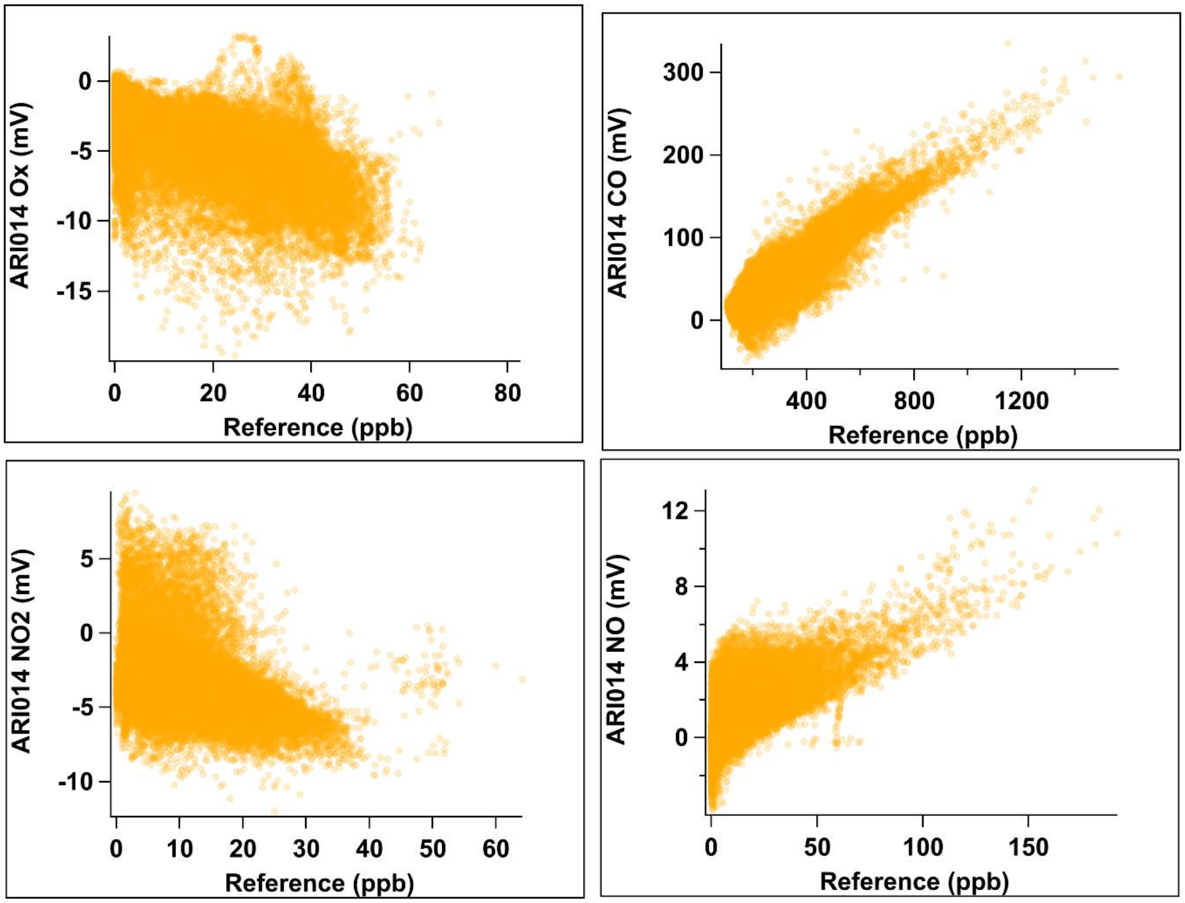

Figure S33: Scatter plots of raw differential voltage data from each gas sensor in ARI014 (y-axis) compared to reference data (x-axis) during post-deployment collocation in North Carolina.

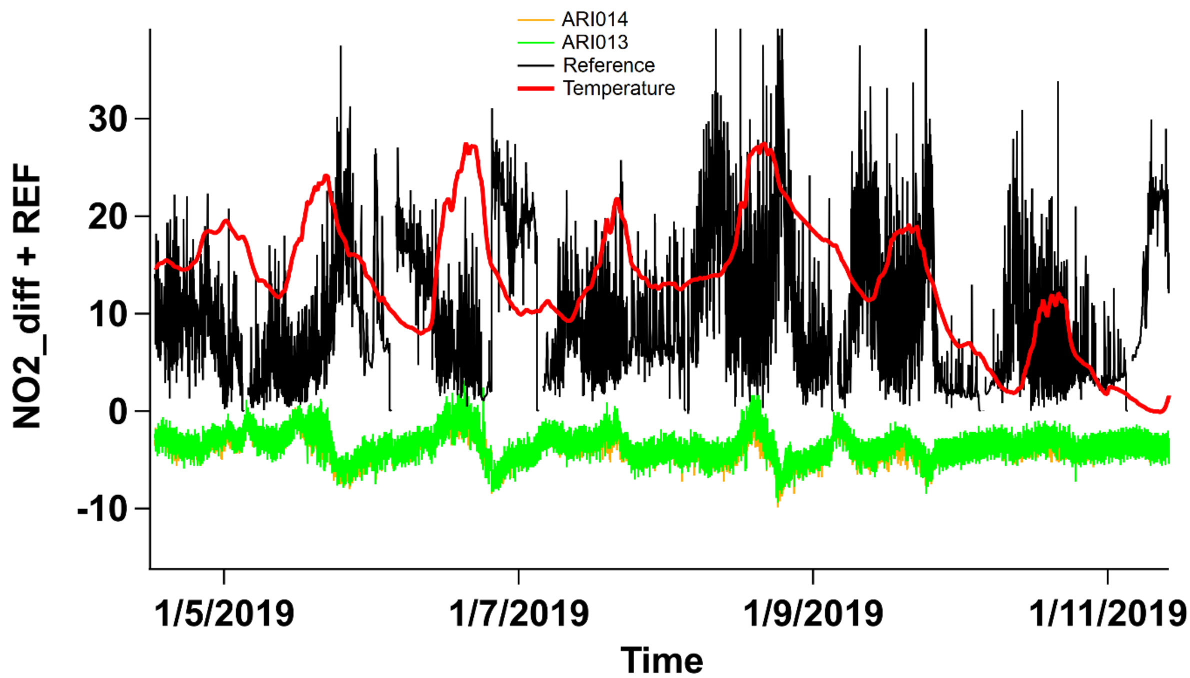

Figure S34: Time series of raw NO_2 differential voltage data from ARI013 and ARI014, NO_2 reference data (black), and temperature (red) during post-deployment collocation in North Carolina.

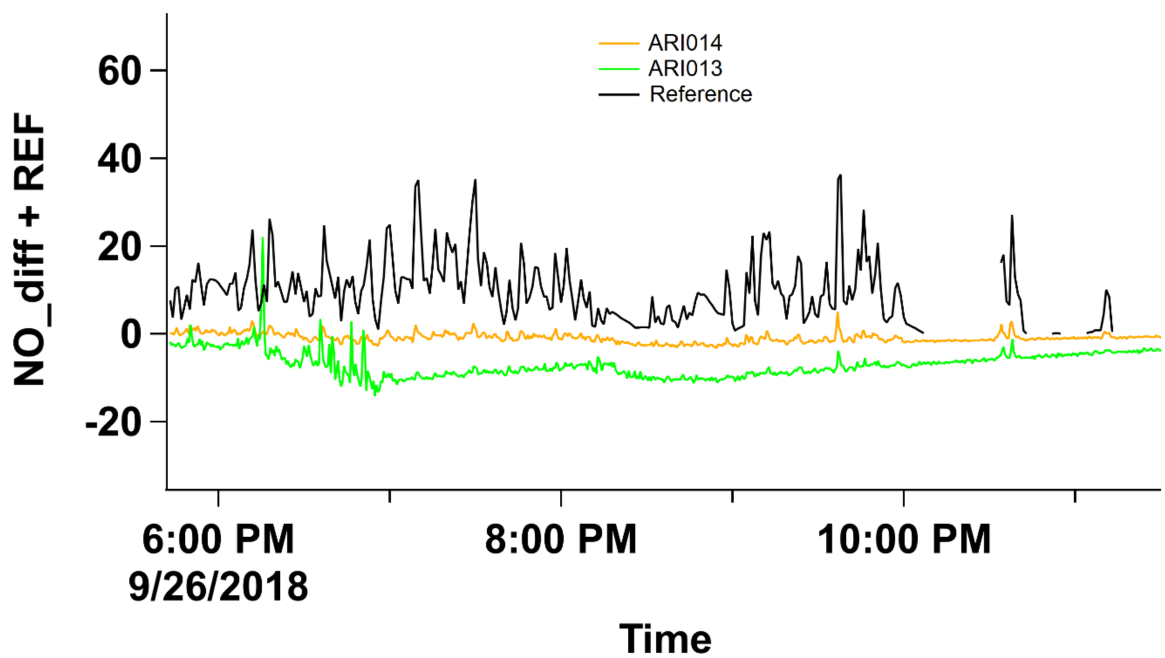

Figure S35: Time series of raw NO differential voltage data from ARI013 and ARI014 and NO reference data (black) during post-deployment collocation in North Carolina.

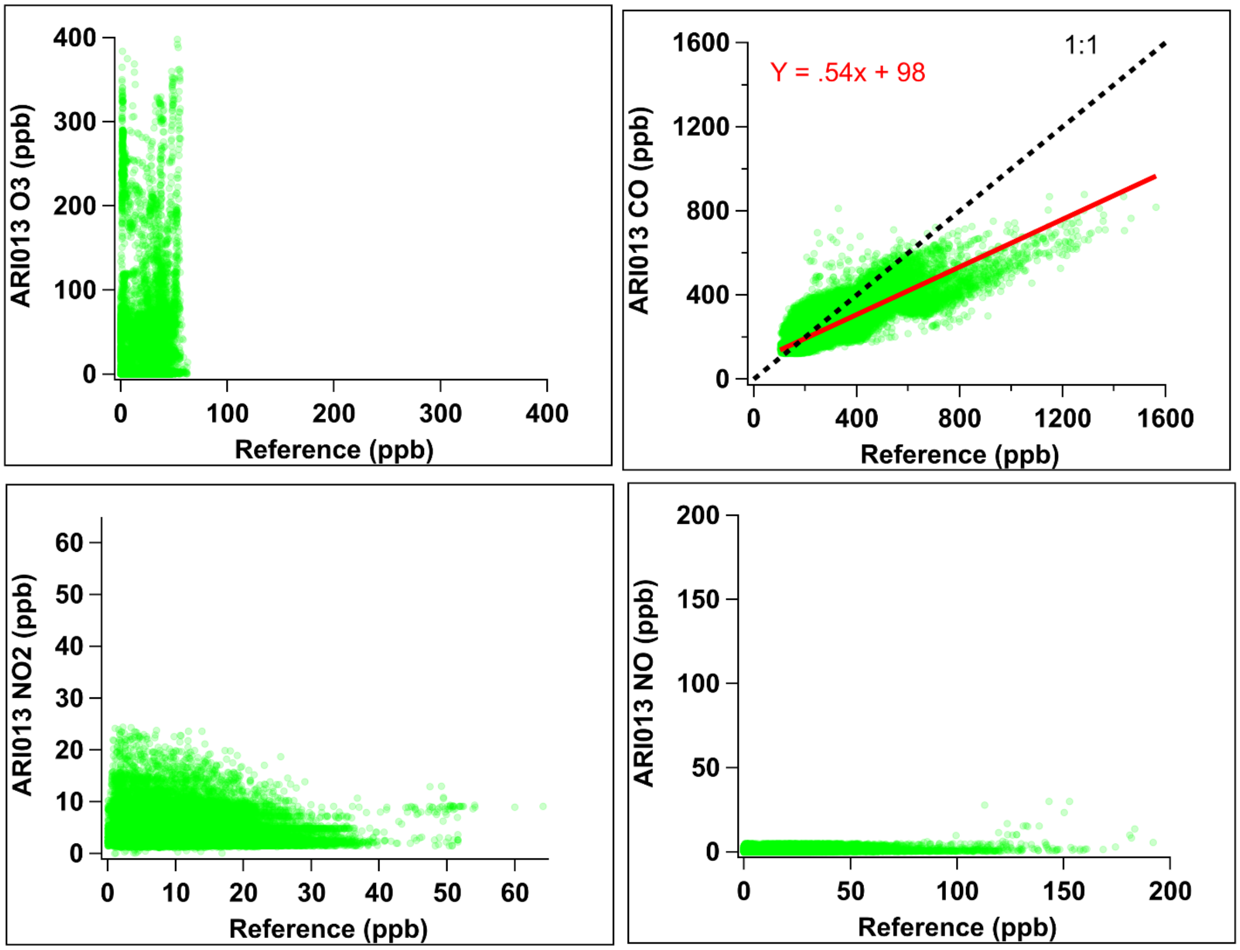

Figure S36: Scatter plots of kNN-calibrated data from each gas sensor in ARI013 (y-axis) compared to reference data (x-axis) during post-deployment collocation in North Carolina. Linear regression coefficients (y = mx + b), fit line (red line), the Coefficient of Determination (R^2) are shown for each paired comparison; A one to one comparison line is shown as the dotted black line.

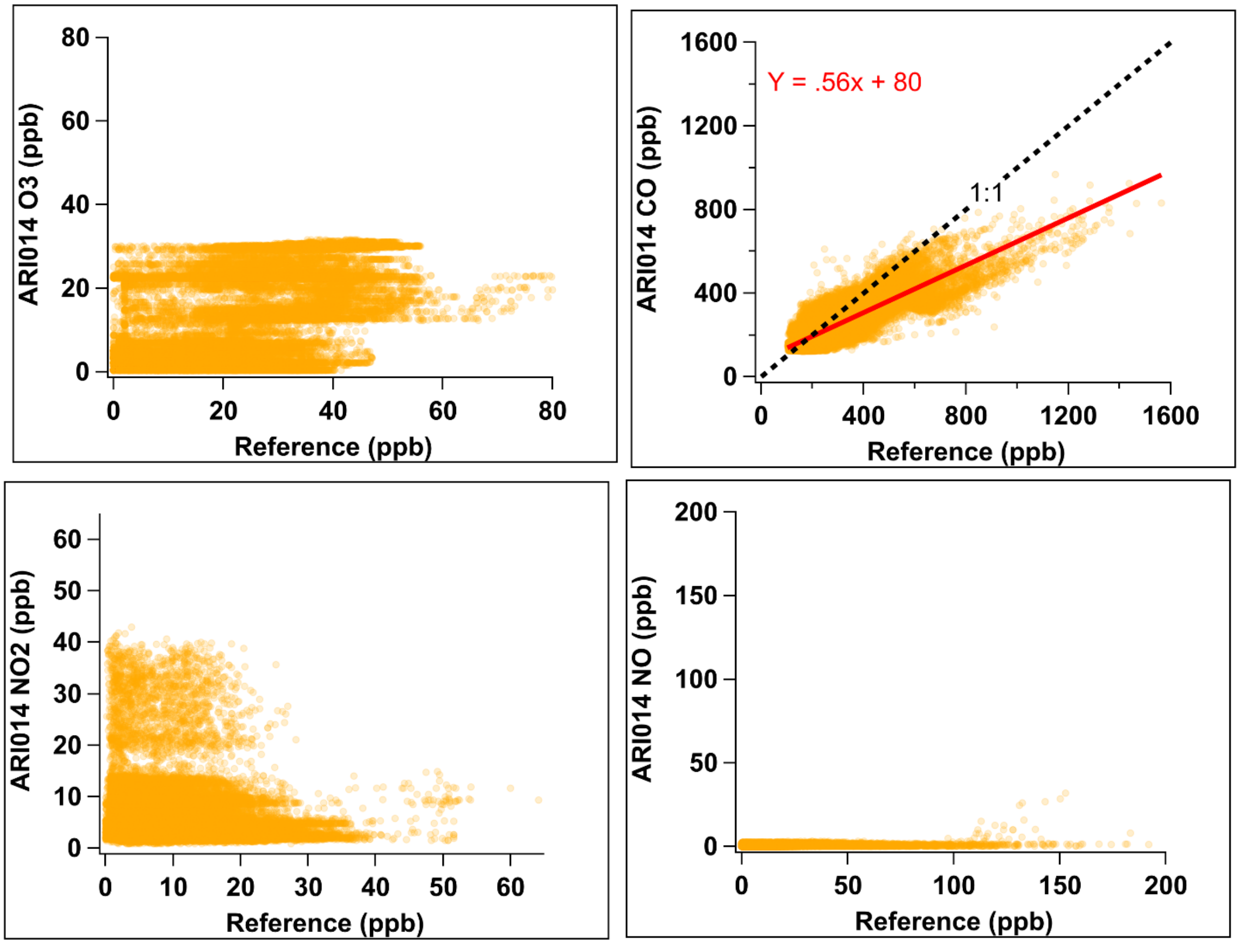

Figure S37: Scatter plots of kNN-calibrated data from each gas sensor in ARI014 (y-axis) compared to reference data (x-axis) during post-deployment collocation in North Carolina. Linear regression coefficients (y = mx + b), fit line (red line), the Coefficient of Determination (R^2) are shown for each paired comparison; A one to one comparison line is shown as the dotted black line.

Table S7: Performance metrics for ARISense 013 and 014 during post-deployment collocation with reference instruments in NC. Values are shown for each of the four gas sensors and for each calibration model assessed in this study. R^2 = Coefficient of Determination, MAE = mean absolute error, CO = carbon monoxide, NO = nitric oxide, NO2 = nitrogen dioxide, O3 = ozone.

Final Round (Post collocation)	**ARI013**		**ARI014**	
	MAE (ppb)	**R^2**	**MAE (ppb)**	**R^2**
CO				
HDMR	100.	0.25	105.	0.22
MLR	100.	0.25	105.	0.22
kNN Hybrid	68.6	0.57	72.2	0.55
RF Hybrid	67.7	0.55	73.6	0.51
QR	143.	-0.45	142.	-0.38
NO				
HDMR	28.0	-4.14	23.9	-2.46
MLR	13.5	-0.39	16.0	-0.69
kNN Hybrid	11.4	-0.39	11.6	-0.43
RF Hybrid	10.4	-0.12	10.8	-0.10
NO2				
HDMR	10.7	-2.27	9.29	-1.91
MLR	13.6	-4.05	13.4	-4.58
kNN Hybrid	6.97	-0.72	7.31	-1.06
RF Hybrid	5.72	-0.31	5.61	-0.19
O3				
HDMR	45.5	-28.7	82.6	-42.0
MLR	32.4	-8.94	49.3	-13.5
kNN Hybrid	26.9	-7.00	12.4	-0.15
RF Hybrid	58.0	-962.	16.1	-0.80

References

Badura, M., Batog, P., Drzeniecka-Osiadacz, A., and Modzel, P.: Evaluation of Low-Cost Sensors for Ambient PM2.5 Monitoring, J. Sensors, vol. 2018, Article ID 5096540, 16 pages, https://doi.org/10.1155/2018/5096540, 2018.

Box, G. E. P. and Cox, D. R.: An Analysis of Transformations, J. Roy. Stat. Soc. B Met., 26, 211–252, 1964.

Bulot, F. M. J., Johnston, S. J., Basford, P. J., Easton, N. H. C., Apetroaie-Cristea, M., Foster, G. L., Morris, A. K. R., Cox, S. J., and Loxham, M.: Long-term field comparison of multiple low-cost particulate matter sensors in an outdoor urban environment, Sci. Rep-UK, 9, 7497, https://doi.org/10.1038/s41598-019-43716-3, 2019.

Champion, W. M. and Grieshop, A. P.: Pellet-fed gasifier stoves approach gas-stove like performance during in home use in Rwanda, Environ. Sci. Technol., in press, acs.est.9b00009, https://doi.org/10.1021/acs.est.9b00009, 2019.

Crilley, L. R., Shaw, M., Pound, R., Kramer, L. J., Price, R., Young, S., Lewis, A. C., and Pope, F. D.: Evaluation of a low-cost optical particle counter (Alphasense OPC-N2) for ambient air monitoring, Atmos. Meas, Tech., 11, 709–720, https://doi.org/10.5194/amt-11-709-2018, 2018.

Duvall, R., Clements, A., Hagler, G., Kamal, A., Vasu Kilar, Goodman, L., Frederick, S., Johnson Barkjohn K., VonWald, I., Greene, D., and Dye, T.: Performance Testing Protocols, Metrics, and Target Values for Fine Particulate Matter Air Sensors: Use in Ambient, Outdoor, Fixed Site, Non-Regulatory Supplemental and Informational Monitoring Applications, U.S. EPA Office of Research and Development, Washington, DC, 2021a.

Duvall, R., Clements, A., Hagler, G., Kamal, A., Vasu Kilar, Goodman, L., Frederick, S., Johnson Barkjohn K., VonWald, I., Greene, D., and Dye, T.: Performance Testing Protocols, Metrics, and Target Values for Ozone Air Sensors: Use in Ambient, Outdoor, Fixed Site, Non-Regulatory and Informational Monitoring Applications, U.S. EPA Office of Research and Development, Washington, DC, 2021b.

Rai, A. C., Kumar, P., Pilla, F., Skouloudis, A. N., Di Sabatino, S., Ratti, C., Yasar, A., and Rickerby, D.: End-user perspective of low-cost sensors for outdoor air pollution monitoring, Sci. Total Environ., 607–608, 691–705, https://doi.org/10.1016/j.scitotenv.2017.06.266, 2017.